**TH-PM-1S** CHEMICAL LABELING AND THE GEOMETRY OF MEMBRANE PROTEINS. F.M. Richards, Department of Molecular Biophysics and Biochemistry, Yale University, New Haven, Conn. 06520.

A brief survey of vectorial labeling procedures shows that no single technique or reagent, so far reported, is a reliable general indicator of the position of protein components with respect to the plane of the bilayer. Standard protein labeling reagents are plagued with the problems of specificity based on both size and reactivity. Photochemically induced reactive species have an equivalent but different set of problems. Results on the erythrocyte membrane will be used to provide examples of the types of information that can be obtained and some of the anomalies involved.

The two-dimensional arrangement of the proteins in the plane of the membrane can be assessed by crosslinking with bifunctional reagents. These reagents have all the difficulties inherent in the monofunctional species referred to above. In addition the interpretation of the results must cope with the problem of molecular motion. Simple oligomeric macromolecules or even more complex organelles such as ribosomes can assume statis structures in dilute solution for periods long enough to carry out crosslinking reactions. Observed complexes can usually be interpreted unambiguously. The total membrane protein represents a concentrated two-dimensional solution. The fluidity of the bilayer may permit rapid motion on a molecular level. The distinction between stable and collision complexes thus becomes difficult on the basis of any single crosslinking experiment. Data with various reagents will be discussed in terms of the complexes observed and their significance.

**TH-PM-2S** THE MOBILITY OF A GLYCOPROTEIN RECEPTOR ON CELL SURFACES. J. Schlessinger[1], School of Applied and Engineering Physics, and Department of Chemistry, Cornell University, Ithaca, New York 14853

The apparent mobility of glycoprotein receptors on the surface of cultured rat myoblasts has been measured by observing the kinetics of the local recovery of the fluorescence of labeled lectin receptors due to lateral transport following photobleaching.[2] The receptors are tagged with rhodamine labeled tetravalent concanavalin A (Con A) or divalent succinyl concanavalin A (S-Con A). Binding of the lectin is followed by aggregation involving the Con A molecules and receptors leading to patch formation; some patches seem to be mobile. The rate of fluorescence recovery is strongly dependent on the Con A dose and valence, decreasing as aggregation proceeds. The mobility of receptor tagged with divalent S-Con A slows with time after incubation but never ceases as in the case of intact tetravalent Con A. Further evidence that the aggregation process is the cause of the reduction with time of receptor mobility is manifested by complete abolishment of both S-ConA and Con A mobility by binding of Anti-Con A, which cross links adjacent lectin molecules. Furthermore, the extrapolated mobilities of S-Con A and Con A at short times after incubation are rather similar, suggesting similar degrees of short time aggregation. The effect of treatments and drugs that are known to affect cell activity were examined. For example, azide, colchicine, and incubation at low temperature do not seem to affect the lectin mobility; while cell temperature during recovery is a factor. The relationship between receptor mobility diffusion and cell movement will be discussed.

[1]Collaborators include: D.E. Koppel, D. Axelrod, K. Jacobson, E.L. Elson and W.W. Webb.
[2]See poster presentations by D. Axelrod et al., and by D.E. Koppel et al.

**TH-PM-4S** CELL MEMBRANE ASSOCIATION WITH CYTOPLASMIC COMPONENTS. Keith R. Porter, MCD Biology, University of Colorado, Boulder, Colorado 80302

Just inside the unit membrane, i.e. the bimolecular leaflet limiting the cell, there is ordinarily a layer of cytoplasm called the cytoplasmic cortex that is strongly adherent to and essentially an integral part of the inner surface of the leaflet. It is a finely fibrous layer that achieves an extraordinary thickness (1.0-2.0 μm) as the terminal web in the absorptive cells of the intestinal epithelium but finds some expression in all cells. Actin and spectrin can be isolated from the cortex as it occurs in the ghosts of red blood cells and evidence of myosin plus actin is available in the case of the terminal web. In intact whole cells, observed by high voltage microscopy, the cortex can be seen to be confluent with bundles of actin filaments, with arrays of microtubules and with microtrabeculae that extend from the cortex into the deeper regions of the cytoplast. This talk will review the evidence for the presence and distribution of these elements as part of the cytoplasmic cortex as well as comment on their probable function.

TH-PM-A1 PRELIMINARY REPORT ON AN ACTIN-LIKE PROTEIN IN E. COLI AND THE CYTOTONUS CONCEPT. L. Minkoff and R. Damadian, Department of Medicine and Program in Biophysics, State University of New York at Brooklyn, Brooklyn, New York 11203.

We wish to report the isolation of an actin-like protein from E. coli. The protein was first extracted from E. coli by an acetone powder technique used in the isolation of skeletal muscle actin. This protein fraction (A-L fraction) undergoes reversible increases in molecular weight under the same catalytic conditions that polymerize actin. The fraction exhibits a distinct peak by SDS electrophoresis at the characteristic molecular weight of actin. Passage of skeletal muscle myosin through A-L fraction specifically removes this band. Examination of the myosin by SDS electrophoresis after passage exhibits a new band at the molecular weight of actin. Growth of E. coli in uniformly labeled $C^{14}$ glucose to mark all cell proteins demonstrated that all of the radioactivity transferred to the myosin-E. coli protein complex was concentrated in the 45,000 molecular weight band. Careful study of the organism from which it was extracted established that it could not be involved in locomotion since the organism was non-motile. It seemed to us that it might act to maintain a type of "tonus" at the microscopic level analogous to the well-known tonus of macroscopic tissues.

TH-PM-A2 ACTIN IN MAMMARY TUMOR VIRUS. C. H. Damsky, G. P. Tuszynski*, J. B. Sheffield* and L. Warren.* The Wistar Institute, 36th and Spruce Sts., Philadelphia, Pa. and The Institute for Medical Research, Camden, New Jersey.

The murine mammary tumor virus (MuMTV) is an RNA-containing, enveloped, oncornavirus which can be isolated from the milk of infected mice or from the fluids of cultured mammary tumor cells. A protein comigrating with purified chick muscle actin is observed when gradient purified MuMTV is separated using SDS discontinuous polyacrylamide gel electrophoresis. The protein comprises 1-2% of the virus protein. To demonstrate that the protein in question is indeed an actin, the protein was first eluted from a stained and fixed SDS preparative slab gel of MuMTV. The SDS was then removed from the protein by electrodialysis in the presence of 8M urea and the SDS-free protein was run on an acid-urea continuous polyacrylamide gel system in a sample buffer containing 5% triton, 5% acetic acid, 5% mercaptoethanol pH 2.5. The putative virus actin comigrated with both chick muscle actin which had undergone the same processing procedure, and chick muscle actin which had not been run on an SDS gel. Since there is a major protein component in both virus-free mouse milk and tissue culture fluid which comigrates with actin, it is essential to rule out the non-specific binding of an actin-like protein to the outside of the virus during isolation. Labeling studies on intact and disrupted virus using $^{125}I$ iodine indicate that most, if not all, the actin is located inside the virus particle. MuMTV particles are released into the lumen of the mammary gland from the ends of long microvilli. Bundles of microfilaments are visible within these microvilli and can be seen to impinge on the virus particles at the ends of the microvilli. Whether actin plays a role in transport of incomplete particles to the cell membrane, virus release or virus infectivity is at present unknown. Supported by PHS grants 5-T01-6M-00849, CA-08740, NIH grants CA-19130-01, 1-F02-AM-55449-01.

TH-PM-A3 CONTRACTILE PROTEINS IN NORMAL AND TRANSFORMED FIBROBLASTS. J.E. Schollmeyer*, G. Wendelschafer-Crabb*, and L. T. Furcht* (Intr. by E.S. Benson), University of Minnesota, Minneapolis, MN 55455.

Increasing evidence suggests that contractile proteins may play a role in the phenomenon of contact inhibition. Our ultrastructural studies and previous work by McNutt et al demonstrate that the 60-80 Å and 100 Å microfilaments in normal 3T3 cells are frequently aggregated into meshworks which stream through the cytoplasm in parallel arrays that appear to coalesce in a number of densely stained areas near the plasma membrane. SV3T3 transformed fibroblasts, on the other hand, demonstrate fewer microfilament sheets, and they do not appear to coalesce into dense regions adjacent to the plasma membrane. We have performed immunocytochemical localization of contractile proteins known to be associated with the microfilament sheets in an attempt to determine the role that these proteins may play in determining the behavior of normal and transformed cells in vitro. We have utilized α-actinin and tropomyosin isolated from chicken gizzard to which monospecific, as determined by immunoelectrophoresis, Fab antibody fragments were prepared in rabbits. Cells were then reacted with either fluorescein or peroxidase conjugated sheep anti-rabbit Fab and were then viewed by fluorescence or electron microscopy. In normal cells a highly organized staining pattern was observed for α-actinin and tropomyosin; conversely, in the transformed cells, the staining pattern exhibited no significant organization and was visualized as a generalized diffuse staining. These studies suggest that there are fundamental differences in the distribution and membrane association of these contractile proteins in normal and transformed or malignant cells. (Supported in part by grants from the NIH/NCI and the Minnesota Medical Foundation.)

TH-PM-A4 THE GELATION AND CALCIUM SENSITIVE MOVEMENTS IN EXTRACTS FROM AMOEBA PROTEUS AND DICTYOSTELIUM DISCOIDEUM. John S. Condeelis and D. Lansing Taylor. The Biological Laboratories, Harvard University, Cambridge, Mass.

Calcium sensitive motile extracts of A. proteus and Dictyostelium discoideum have been prepared by fractionating mass cultures in either a stabilization or a relaxation solution (Taylor et al. J. Cell Biol. 67: 427a 1975). The addition of a contraction solution to extract I induced a rapid gelation followed by contractions. SDS gel electrophoresis demonstrated the presence of actin, myosin, 55,000, 95,000, 280,000 M.W. bands and polypeptides that comigrate with bands 1 and 2 from red blood cell ghosts (spectrin). Negatively stained preparations contained actin filaments, myosin aggregates, amorphous aggregates, fibrous aggregates that did not label with HMM and structures identical morphologically to particles isolated from red blood cell ghosts by Harris( J. Mol. Biol. 46: 329, 1969). The extracts were transformed from the non-motile unstructured state to the geled state and the geled-contracted state by varying the calcium and Mg-ATP concentrations. The transition from non-motile to motile extracts involves at least a two step process involving the transformation of actin from a non-filamentous to a filamentous state and the contraction of actin and myosin. (Supported by research grant AM 18111 from the National Institute of Arthritis, Metabolism, and Digestive Diseases to D. L. T.).

TH-PM-A5 MICROFILAMENTS IN THE SEA URCHIN EGG AT FERTILIZATION. P. Kidd, G. Schatten, J. Grainger, and D. Mazia. Dept. Zoology, Univ. Calif., Berkeley, Ca. 94720. (Intr. by L. Lemanski).

Microfilaments are associated with the inner plasmalemmal face of fertilized or activated Lytechinus eggs, examined by TEM and SEM. Isolated egg surfaces were glued to polylysine-coated glass or resin surfaces (Schatten and Mazia, Exp. Cell Res., in press). 1. UNFERTILIZED surfaces consist of the plasmalemma with attached vitelline layer, and cortical granules on its inner (cytoplasmic) face. 2. FERTILIZED surfaces lack cortical granules; they consist of plasmalemma with 5-8nm diameter filaments attached to its inner face; in the SEM, these often appear as 50-200nm bundles associated with the entering spermatozoon. Some fertilization-associated activities can be turned on by immersing the egg in a nonelectrolyte, such as iso-osmotic glycerol (Mazia et al, PNAS 72 (11) ). 3. Such ARTIFICIALLY ACTIVATED surfaces isolated from glycerol closely resemble fertilized surfaces, also bearing 5-8nm filaments. Glycerol-treated eggs contract dramatically when returned to sea water; these contracting eggs contain bundles of subplasmalemmal 5-8nm filaments. The 5-8nm filaments of our study may contain actin, which is often associated with isolated plasmalemmas. There is difficulty in preserving microfilaments in intact eggs, perhaps due to disassembly during fixation or inability to discern filaments not arranged in bundles. Here the egg surface complex was freed from cytoplasm before fixation, and the filaments were preserved. The roles of microfilaments in fertilization could include facilitating sperm entry, and establishing the block to polyspermy. Supported by NIH grant GM-13882 to Dr. Mazia.

TH-PM-A6 ISOLATION AND CHARACTERIZATION OF AN ACTIN-LIKE PROTEIN FROM HUMAN ERYTHROCYTE MEMBRANES. Tsuyoshi Ohnishi, Dept. of Anesthesiology Biophysics Laboratory and Dept. of Biological Chemistry, Hahnemann Medical College, Philadelphia, Pa. 19102

An actin-like protein in erythrocyte membranes was first found by the author(J.Biochem.52,307(1962)), and the name of erythro-actin was proposed. Recently, several authors have discussed the existence of the protein(Singer,S.J:Ann.Rev.Biochem.43,805(1974), Haley,B.E.et al.:Proc.Nat.Acad.Sci. USA.71,3367(1974), Avissar,N. et al.:Biochim.Biophys.Acta 375,35(1975) and Kirkpatrick,F.H.et al.1975 Biophysics Meeting).

The existence of erythro-actin was confirmed this time by the following experiments: Erythro-actin was extracted from acetone-treated ghost and purified by ammonium sulfate fractionation. Erythro-actin undergoes G-F transformation and forms filaments on addition of 0.1 M KCl. The filaments can be decorated by muscle heavy-meromyosin. Erythro-actin and muscle actin have the same molecular weight. At high ionic strength, the hybrid of erythro-actin and muscle myosin shows the viscosity drop phenomenon on addition of ATP. At low ionic strength(0.045 M KCl), erythro-actin enhances myosin ATPase eleven times. Superprecipitation is also observed under this condition.

All these properties confirm that erythro-actin closely resemble muscle actin.

TH-PM-A7 SPIN LABEL STUDIES OF THE INTERACTION OF SPECTRIN WITH ACTIN AND WITH LIPOSOMES. F.H. Kirkpatrick, Department of Radiation Biology & Biophysics, University of Rochester School of Medicine and Dentistry, Rochester, NY 14642

Spectrin was extracted from human erythrocyte ghosts by dialysis against 0.1 mM EDTA and concentrated by precipitation at pH 5.1. Actin was extracted from rabbit acetone powder and purified (J. Biol. Chem. 246:4866, 1971). F-actin was spin labelled with piperidine-maleimide spin label and was purified by two further cycles of polymerization-depolymerization; EPR spectra were comparable to literature reports. Stock solutions of proteins (10 mg/ml) and cations were mixed in various orders to obtain final concentrations: 1.6 mg/ml actin, 8.0 mg/ml spectrin, 50 mM KCl, 3 mM $CaCl_2$. Addition of spectrin to G-actin gave no change in EPR spectra, while polymerization of G to F with KCl immobilized the label. Spectrin partially mobilized the label on F-actin. Effects with calcium depended on the order of addition of the reagents in a complex manner. The mode of interaction of spectrin and actin appears to depend on the polymeric state of both components.

Whole erythrocyte lipids were extracted with chloroform-methanol, dried, redissolved in chloroform, mixed 50:1 by weight with cholestane spin label, dried, and sonicated with 5 mM HEPES either alone or containing 1 mg/ml of spectrin. Final lipid concentration was 1.5 mg/ml. Pure liposomes showed no EPR spectral changes on addition of 150 mM NaCl, 5 mM $CaCl_2$, or both. Liposomes containing spectrin were identical with pure liposomes in the presence or absence of NaCl, but the correlation time of the labels increased slightly with $CaCl_2$ and significantly with both ions, possibly indicating penetration of spectrin into the hydrophilic region of the bilayer.

This work was supported by NIH grants HL00146-01, HL18208-01, HL16421-05 and by ERDA contract with the U. Rochester BER Project, and has been assigned Report # UR-3460-858.

TH-PM-A8 TWO FORMS OF PLATELET ACTIN DIFFER FROM SKELETAL MUSCLE ACTIN. Michael Gallagher*, Thomas C. Detwiler*, and Alfred Stracher, Dept. of Biochemistry, S.U.N.Y. Downstate Med. Center, Brooklyn, N.Y. 11203.
Intr. by Lawrence Herman.

We have isolated two forms of platelet actin. Neither form has polymerization properties similar to skeletal muscle actin. Type $1_p$ (p=polymer) is not depolymerized by any of the non-denaturing conditions used to depolymerize skeletal muscle actin. Type II is isolated as a monomer in CaATP, 0.5 M KCl. This is a polymerization condition for skeletal muscle actin; sucrose gradients demonstrate this difference. Actin II can be reversibly polymerized by either MgATP-KCl or by KCl alone. Sucrose gradients show that this polymer, in the absence of ATP, binds to both platelet myosin and to platelet myosin head (a proteolytic product of myosin which retains ATPase activity). We conclude that other workers have overlooked the distinctive polymerization properties of platelet actins, and that they are able to purify what we term Type II actin by polymerization-depolymerization cycling despite differences between platelet and muscle actin.

This work was supported by Grant Number HL14020 from the National Heart and Lung Institute and by the New York Heart Association.

TH-PM-A9 MYOSIN PHOSPHORYLATION IN DIVIDING CELLS. S.P. Scordilis and R.S. Adelstein, Section on Molecular Cardiology, NHLI, NIH, Bethesda, Md. 20014

Myosin has been isolated from the following three sources: (1) human rhabdomyosarcoma (a tumor of skeletal muscle); (2)pre-fusion rat myoblasts; and (3) SV40-transformed cultured mouse astrocytic neuroglial cells. Electrophoresis of these myosins in SDS-polyacrylamide gels revealed a heavy chain of 200,000 daltons and light chains of 16,000 and 20,000 daltons. Addition of $MgCl_2$ and $\gamma$-$AT^{32}P$ to the 30-55% $(NH_4)_2SO_4$ fraction of each myosin in 0.5 M KCl resulted in the phosphorylation of the 20,000 dalton light chains. Phosphorylation was mediated by an endogenous kinase in each case. Further evidence for this was obtained for the rhabdomyosarcoma and virally transformed cells by separation of the myosin and kinase by Sepharose 4B gel filtration. The partially purified kinase isolated from these cells resembles the kinase previously isolated from human platelets (Adelstein et al., (1975), Proc. 9th Meeting FEBS, 31: 177-186) in (a) dependence on Mg++ for activity, (b) ability to phosphorylate the 20,000 dalton light chain of platelet myosin, and (c) inability to phosphorylate the 18,500 dalton light chain of human and rabbit skeletal muscle myosins. In contrast to the kinase associated with myosin from these dividing cells and similar to the findings of Pires et al. (FEBS Lett., 41: 292-296, 1974)in rabbit skeletal muscle, normal human muscle was found to contain a kinase capable of phosphorylating the 18,500 dalton light chain of human skeletal muscle myosin. The human skeletal muscle kinase is incapable of phosphorylating the 20,000 dalton light chains of human platelet and SV40-transformed astrocytic neuroglial myosin. (S.P. Scordilis is a Postdoctoral Fellow of the Muscular Dystrophy Association).

**TH-PM-A10** DETECTION OF DIFFERENT CONFORMATIONS IN PLATELET MYOSIN. M. N. Malik*, Paulette J. Kolchin* and A. Stracher, Department of Biochemistry, SUNY, Downstate Medical Center, Brooklyn, New York 11203. (Intr. by H. Schuel).

We have demonstrated the existence of cooperatively interacting ATP (Malik et al. BBBC 55, 912, 1973); and Ca++ (Malik et al. 61, 1071, 1974) binding sites of platelet actomyosin. Recently we have also presented evidence indicating that the ADP binding site of platelet actomyosin is distinct from its catalytic site (Malik et al. Fed. Proceedings 34, 670, 1975; Manuscript in preparation). We now describe a procedure which is straightforward and less time consuming for the preparation of platelet myosin. This method yields homogeneous myosin which is free of platelet actins and other proteins. The kinetics of this isolated platelet myosin ATPase has also been investigated. We have again obtained sigmoidal kinetics suggesting cooperatively interacting ATP binding sites of platelet myosin. In addition, it appears from the kinetic data that platelet myosin possesses two distinct Km values. The significance of these findings may point to the fact that platelet myosin exists in different conformations depending upon the CaATP (substrate) concentration. Supported by grants from the N. Y. Heart Association and HL 14020 from the National Heart and Lung Institute. M. N. M. is an established investigator of the American Heart Association.

**TH-PM-A11 EFFECTS OF DIRECT CURRENT INJECTION ON THE ACTIVITY OF BULL SPERMATOZOA.** **P.M. O'Day, R. Rikmenspoel and C.B. Lindemann, Department of Biological Sciences, SUNY at Albany, Albany, N.Y. 12222.**

**Injection of direct current by KCl filled glass microelectrodes has been used to investigate the control of motility in bull spermatozoa. Negative current decreases the frequency of the flagellar beat. The current necessary to reduce the flagellar beat frequency to one-half of the value prior to injection, $i_{1/2}$, is proportional to the external magnesium concentration up to 2mM Mg: $i_{1/2}$ = -0.07uA for 0.05mM Mg, = -0.38uA for 0.5mM Mg, and = -1.20 uA for 2.0mM Mg. A sharp kink in the midpiece of the flagellum sometimes developed under conditions of high negative current at low magnesium concentrations and moderate positive current at all magnesium contractions. The change in resistance of the electrode due to the impalement of a sperm head, as measured by an a.c. Wheatstone bridge, was (+200 ± 300) kilohms (av. ± S.D.), that due to withdrawing the electrode from the sperm head (-150 ± 200) kilohms (av. ± S.D.). This indicates that the injected negative current may induce a potential in the sperm which is in the physiological range. The overall results are compatible with the concept of a $Mg^{++}$ pump which extrudes $Mg^{++}$ when negative current is injected.**
**Supported in part by NICHD through grant HD-8752.**

**TH-PM-A12** THE CONTRACTILE EVENTS IN THE CILIA OF PARAMECIUM, OPALINA, MYTILUS AND PHRAGMATOPOMA. R. Rikmenspoel, Department of Biological Sciences, State University of New York at Albany, Albany, N.Y. 12222

The motion of the abnormal cilia of Opalina and Mytilus can be described by the recently developed model for ciliary motion (Biophysical Journal, 13, 955, 1973), provided the activation of the contractility during the effective stroke is reduced by 3 to 5 fold compared to that in the recovery stroke. The stiffness of the cilia of Paramecium, Opalina and Phragmatopoma during the entire cycle, and of Mytilus during the recovery phase is predicted correctly by the model. During the effective stroke of the Mytilus cilium the stiffness is found several hundred times larger than that predicted by the model, however. The activation of contractility in Mytilus and Phragmatopoma cilia increases with the viscosity of the medium, as the velocity of the ciliary motion slows down. This leads to the equivalent of a force-velocity relation. The velocity of propagation of the bend in the cilia during the recovery stroke is shown to be dependent only on the elastic properties of the ciliary shaft, and to be independent of the contractile activity. (Supported in part by NICHD through grant HD-6445.)

TH-PM-A13 A PARTIAL INHIBITION OF MOTILITY IN REACTIVATED BULL SPERM USING $NiCl_2$ AND $CuSO_4$. C.B. Lindemann, Biology Dept., Oakland University, Rochester, Michigan, and Robert Rikmenspoel, Biology Dept., State University of New York at Albany, Albany, New York.

Two procedures were employed to disrupt the integrity of the plasma membrane of bull sperm and maintain the motility. In the first procedure the membrane of the sperm was mechanically ruptured by micromanipulation with a glass probe in a bathing solution containing 4mM ADP and 0.5mM $Mg^{2+}$. The second procedure utilized 0.1% Triton X-100 to eliminate the plasma membrane and subsequently 1mM ATP and 1mM $Mg^{2+}$ or 0.1mM ATP, 4mM ADP and 1mM $Mg^{2+}$, was applied. It was necessary to include either 4mM ATP or 1mM dithiotreitol (DTT) to obtain stable motility. The coordinated wave motion of treated cells was inhibited by $Ni^{2+}$ and $Cu^{2+}$. The concentration of $Ni^{2+}$ or $Cu^{2+}$ required to stop coordinated wave formation was a function of the concentration of ADP and DTT in the medium. At the concentrations of ADP and DTT which we employed, 0.3mM $Ni^{2+}$ stopped motility after either of the above treatment procedures, whereas 0.5mM $Cu^{2+}$ stopped motility of the Triton treated cells only. After $Cu^{2+}$ or $Ni^{2+}$ treatment bull sperm could be made to reassume coordinated motion by bending the flagellum and restraining the tip of the flagellum with a microprobe. The motion lasted as long as the tip of the flagellum remained constrained by the probe, and could be turned on and off by alternately restraining and releasing the flagellum. The sperm neither lost their ability to respond to mechanical restraint nor did they appear to diminish in the energy of their response at 20 minutes after the addition of $Ni^{2+}$. We conclude that $Cu^{2+}$ and $Ni^{2+}$ ion can affect sperm by inhibiting the native ability to coordinate wave motion while the capacity to generate force is retained. Supported by NIH Grant HD 08752.

TH-PM-A14 CONTROL OF OVIDUCTAL CILIARY ACTIVITY. EFFECT OF EXTRACELLULAR $[Ca^{2+}]$. W.I. Lee, P. Verdugo, J.M. Schurr and R.J. Blandau*, Center for Bioengineering, Department of Chemistry and Department of Biological Structure, University of Washington, Seattle, Wash., 98195.

Using the frequency of ciliary beat (FCB) as an index of activity, the technique of Intensity Fluctuation Spectroscopy (IFS) was applied to study the effect of $[Ca^{2+}]$ on the ciliary activity of tissue cultures of the rabbit oviduct. Ciliated epithelium of the fimbria were grown in Rose Chambers using modified Eagle's medium with 10% horse serum. The cultures were illuminated by laser beam. The scattered light was collected with heterodyne arrangement by a photomultiplier tube. The autocorrelation function of the photocurrent gives FCB as well as the coherence of ciliary movements. The effect of $[Ca^{2+}]$ on FCB was studied using IFS, high speed film and photometric monitoring. Results obtained using the same experimental protocol show statistical agreement between these methods. Upon introducing a Ca-free Hanks' solution containing 2 mM EDTA into the chamber, FCB slowed down and gradually ceased. Results obtained by equilibrating the cultures in Hanks' solution with different $[Ca^{2+}]$ are shown in Table 1. The evidence presented indicates the existence of one or more calcium dependent processes in the contractile activity of the cilia of the rabbit oviduct.

Supported by grant GM-1643 and grant HD-3752, and contract HD3-2788 from NIH.

Table 1. Effect of $[Ca^{2+}]$ on FCB** at 37°C.

| $[Ca^{2+}]$, mM | 0.001 | 0.01 | 0.1 | 1.0 | 1.5 | 2.5 | 4.0 | 5.0 |
|---|---|---|---|---|---|---|---|---|
| FCB, Hz # | 2.5±2.0 | 15.1±0.8 | 19.6±0.6 | 20.2±1.0 | 20.2±0.7 | 21.0±1.1 | 18.2±1.0 | 18.7±0.9 |

**Each FCB was averaged over 125 sample sites. # Average±SEM.

TH-PM-A15 CONTROL OF OVIDUCTAL CILIARY ACTIVITY. EFFECT OF PROSTAGLANDINS $E_2$. P. Verdugo, W.F. Lee, R.E. Rumery* and P.Y. Tam* Center for Bioengineering and Dept. of Biological Structure, University of Washington RK-15, Seattle, Washington 98195.

The effect of Prostaglandins $E_2$ ($PGE_2$) on ciliary activity and its relationship with extracellular $[Ca^{2+}]$ was studied in tissue cultures of the rabbit oviduct. Ciliated cells of the rabbit fimbria were transplanted to Rose chambers and cultured in modified Eagle's medium. High speed film and laser Intensity Fluctuation Spectroscopy (IFS) were used to assess the frequency of ciliary beat (FCB). When cultures were equilibrated in Hanks' solution with various $[Ca^{2+}]$ and containing $10^{-7}$ M $PGE_2$, a calcium-dependent potentiating effect of $PGE_2$ on ciliary activity was observed. A biphasic time-dependent decrease on FCB was recorded when Ca-free Hanks' solution (Ca-FHS) with 2 mM EDTA was infused into the Rose Chamber. An initial decay to 51.3±3.6%SEM of the control FCB was measured in the first 15 to 20 minutes. During the next 10-15 minutes FCB remained relatively constant, and then rapidly decayed to 25.8±1.6%SEM of the control. This affect was reversible and a similar, although opposite and rather faster affect, was observed when normal 1.25 mM $[Ca^{2+}]$ Hanks'solution was reinfused into the culture chamber. The time course of the changes of FCB in both calcium withdrawal and calcium recharge became much faster and the plateau phase almost disappeared when $10^{-6}$ M $PGE_2$ was added to the Ca-FHS or to the normal 1.25 mM $Ca^{2+}$ Hanks' solution respectively. Furthermore cultures with very low FCB induced by calcium depletion showed a characteristic fast increase followed immediately by a rapid decrease when perfused with a Ca-FHS containing $10^{-6}$ M $PGE_2$. These results show that calcium has a rgulating role in ciliary activity, and suggests the existence of two or more cellular storage sites for calcium. It also indicates that the potentiating effect of $PGE_2$ on ciliary activity seems to be related to calcium release from binding sites within the ciliated cell. Supported by NIH Grant #GM-1643 and Contract HD3-2788.

**TH-PM-A16** EXPERIMENTAL CONTROL OF FLAGELLA PHASE VARIATION IN A SALMONELLA MUTANT. Bernard R. Gerber and Powel H. Kazanjian*. Departments of Physical and Organic Chemistry and Biochemistry, SUNY Downstate Medical Center, Brooklyn, N.Y. 11203.

We report the properties of a mutant organism which appears well-suited to studies on the molecular mechanism for flagella phase variation and so can serve as model for understanding gene-gene interactions. Strain SJ770 is a diphasic mutant of Salmonella typhimurium TM2 which, in phase 2, is non-motile and has straight flagella with H-antigen type 1,2. When cultivated in ten-fold dilute media, however, approximately 50% of these bacteria gradually became motile; their flagella were antigen type i and had a helical shape with pitch of 2.5 μm. At 25°C, 25% of SJ770 cells became motile in approximately 25 h; at 37°C, the same fraction did so in 12 h. On conversion these times corresponded to nearly 5 cell generations at the respective temperatures. The phenomenon is reversible since an increase in nutrient concentration to the standard concentration caused populations of cells gradually to lose motility and regain H-antigen type 1,2. Furthermore, treatment with 0.5 μM chloramphenicol prior to the 5th cell division prevented the initiation of bacterial motility although additions at later times affected neither the mean cell velocity nor the fraction of motile cells. These results and the differences found in flagellar morphology and the serological typing of cells in motile and non-motile stages indicate that the movement observed is due to the synthesis of new flagella. Finally, phase variation of SJ770 flagella also could be produced, even in standard cultural conditions, by the addition of adenosine 3'5'-cyclic monophosphate ($>10^{-4}$ M). Mechanisms are considered which can accommodate these results.

This work has had support by National Science Foundation Grant GB 29367.

TH-PM-B1 ONSET OF MECHANICAL CHANGE FOLLOWING STIMULATION IN FROG STRIATED MUSCLE. Jay B. Wells, Medical Neurology Branch and Laboratory of Biophysics, National Institute of Neurological, Communicative Disorders and Stroke, NIH, Bethesda, Maryland 20014

The first sign of contractile response after electrical stimulation of muscle is an increased stiffness preceding tension development. Measurements of this early stiffness were made to help establish the sequential order of excitation-contraction coupling (ECC) processes. Brief stretches of constant amplitude and duration, 0.4 mm (about 3% $L_o$) or less and 0.3 msec or less, were applied to one end of small bundles of isolated semitendinosus fibers at various times after stimulation. An increased tension response to the applied stretches, recorded at the other end of the muscle, indicated the increased stiffness. The time from stimulus to the first appearance of increased stiffness ($T_s$) for eight preparations at 26° C was 2.00 ± 0.60 msec (mean ± SD) and active tension development ($T_p$) occurred 3.15 ± 0.52 msec after stimulation. The increased stiffness observed above was coincident with latency relaxation (decreased tension and sarcomere elongation) and suggests the occurrence of structural conformations such as cross-bridge formation. At 6°C both time periods were prolonged and the ratio $T_s/T_p$ was 0.63 (n=7) which was similar to the corresponding ratio at 26° C of 0.65. Substitution of normal Ringer bath with $HNO_3$ - Ringer is known to potentiate the twitch response of muscle by lowering the mechanical threshold for activation. Three preparations subjected to this treatment showed no change in $T_s$ or $T_p$. However, substitutions of normal Ringer bath with Ringers made from 99.8% $D_2O$ instead of water increased both $T_s$ and $T_p$. The above results establish the time from stimulus to the first appearance of mechanical contraction. Also, the effects produced by the potentiating agents $NO_3$ - $D_2O$ and decreased temperature support the suggestion that the increased stiffness reflects crossbridge formation during EC coupling processes.

TH-PM-B2 MECHANICAL PROPERTIES OF RELAXING FROG SKELETAL MUSCLE AFTER ISOTONIC TETANIC CONTRACTION. R. T. Hsieh, Department of Biology, Rensselaer Polytechnic Institute Troy, N.Y. 12181

Mechanical properties of relaxing frog sartorius muscle after isotonic tetanic contraction were studied. It was found that (1) during earlier lengthening, the muscle was able to bear tension greater than if it were during an isometric tetanic relaxation at the same length, (2) a sharp decrease of tension occured when the muscle lengthened to its initial length, (3) a period of tension oscillation and (4) steady decay of tension. The effects of temperature and of twitch potentiators were also studied. There was a tension increase after the oscillation at temperatures near 10°C at light loads. The tension increase and the oscillation both disappeared at temperatures near 0°C. Twitch potentiators were able to prolong the relaxation processes however they did not change these properties significantly. Explaination to these mechanical properties of relaxing frog skeletal muscle will be discussed interms of sliding filament hypothesis.

( A part of this work was done in the Division of Physiology, Institute for Muscle Disease, New York. Supported by Muscular Dystrophy Association of America.)

TH-PM-B3 STATIC MECHANICAL BEHAVIOR OF SKINNED SKELETAL AND GLYCERINATED SKELETAL AND CARDIAC MUSCLES. F.J. Julian, R.L. Moss* and M.R. Sollins* (Intr. by M. Elzinga), Dept. Muscle Research, Boston Biomedical Research Institute, Boston, MA 02114.

Segments (1-2 mm) from mechanically (Natori, R., Jikei Med. J., 1954, 1, 18) and chemically (Julian, F.J., J. Physiol., 1971, 218, 117) skinned frog skeletal muscle fibers (MS and CS, respectively) were clamped at either end in microjaws. Unless otherwise noted, the apparatus and solutions were as used by Julian (1971). The initial average sarcomere length (SL) was set to 2.3 μ and the striation pattern was continuously monitored. Consistently, the striation register was better preserved in CS fibers. At 20-22°C (HT), initial resting tension (RT) in both MS and CS fibers was low; however, in MS fibers only, large increases in RT were observed when ionic strength (IS) was reduced from control IS (CIS, 100 mM KCl) to low IS (LIS, 50 mM KCl). At 4-6°C (LT), RT was still low in both the MS and CS fibers and LIS relax solution produced small, partly reversible increases in RT. Further, small, partly reversible increases in RT were observed at LT following maximal contraction and relaxation in LIS solutions. The tension-pCa relationships measured for the CS and MS fibers were similar with respect to the pCa's for minimal and maximal contractions, and the small differences between the pCa's associated with these tension levels. Finally, tests of SR function show that Ca releasing agents elicit contraction in MS fibers only. Strips from glycerinated rabbit papillary muscles were also studied. In high pCa solution, RT disappeared only when the strip became slack (SL ≤ 1.75 μ). In the range, 1.75 μ < SL < 2.3 μ, RT increased moderately with increasing SL. RT increased steeply at SL ≥ 2.3 μ. The pCa levels inducing relaxation and strong contraction were similar to those seen with the MS and CS frog skeletal fibers. (Supported by USPHS HL-16606, NSF GB-40978, AHA 73-699, MHA 1183, MDAA, and USPHS fellowship HL-01210 to RLM).

**TH-PM-B4** CALCIUM DEPENDENCE OF THE FORCE RESPONSE TO CONSTANT VELOCITY STRETCHES IN SKINNED SKELETAL AND GLYCERINATED SKELETAL AND CARDIAC MUSCLES. R.L. Moss*, M.R. Sollins* and F.J. Julian, Dept. Muscle Research, Boston Biomedical Research Institute, Boston, MA 02114.

Low velocity ($< 1$ muscle length/sec), small amplitude ($\Delta L < 7\%$) stretches have been applied to mechanically skinned (MS) and glycerinated (CS) frog skeletal muscle fibers and strips from glycerinated rabbit papillary muscles. The effect of calcium on the force response was determined by equilibrating the preparations in solutions of varying pCa. Solutions and apparatus were as before (Julian, F.J., J. Physiol., 1971, 218, 117), with sarcomere length set to 2.3 μ and temperature to 4-6°C. Length ramps were applied randomly with respect to pCa in the range, $7 \leqslant pCa \leqslant 6$, with applications at $pCa \leqslant 8$ interspersed. At $pCa \leqslant 8$ the force varied linearly with amount of stretch, yielding an elastic modulus of about 0.6 kg/cm$^2$ for the MS and CS preps and 1.1 kg/cm$^2$ for the cardiac. For all of the preps, in the range, $7 \geqslant pCa > 6.5\text{-}6.3$, the force response took the form seen in living muscle using similar methods (Hill, D.K., J. Physiol., 1968, 199, 637). Below the pCa at which this Hill response first appears, the modulus (E) calculated from the initial, elastic part of the response increased slightly with decreasing pCa until pCa = 6.5-6.3 and much more rapidly in the range, $6.5\text{-}6.3 \geqslant pCa \geqslant 6$. Early experiments show this rise to be less steep in the cardiac than in the skeletal preps. For resting, electrically excitable fibers, in which the Hill response is present, an E of about 4.7 kg/cm$^2$ was found. These results indicate that the Hill response in some way depends on calcium activation, probably involving attached cross-bridges, as suggested by Hill. The absence of this response in fibers in the high pCa solution implies that the pCa of this solution is greater than that found in living fibers at rest. (Supported by USPHS HL-16606, NSF GB-40978, AHA 73-699, MHA 1183, MDAA, and USPHS fellowship HL-01210 to RLM.)

**TH-PM-B5** DISRUPTION OF THE SARCOLEMMA OF MAMMALIAN SKELETAL MUSCLE FIBERS BY HOMOGENIZATION. B. Krasner and W.G.L. Kerrick. Department of Physiology and Biophysics, University of Washington, Seattle, Washington 98195.

Light homogenization of rabbit skeletal muscle produces longitudinally intact segments of single muscle fibers. The properties of these segments were compared to those of segments which in addition were mechanically split in half to insure disruption of the sarcolemma. Both groups of fibers gave the same steady-state tension response curve to changes of calcium concentration in the bathing medium. The steady-state tension response curve of homogenized fibers to calcium concentration changes was the same whether sodium of potassium was the major cation constituent of the bathing medium. In addition stimuli which cause rapidly developing tension transients in skinned fibers such as rapid substitution of chloride anion for propionate, or sodium cation for potassium, and rapid increases in free calcium concentration (all done in the presence of 50 μM EGTA) cause rapidly developing tension transients in homogenized fibers (these stimuli do not lead to tension development in intact muscle). Caffeine also causes tension transients. Finally parvalbumin a 10,000 MW protein which can act as a calcium chelator, is able to inhibit like EGTA the response to caffeine caused by release of intracellular calcium. Because of the similarities in the behavior of homogenized and skinned fibers, which differs significantly from that of intact fibers, and because of the apparent permeability to large molecules, it is concluded that homogenized fibers are functionally skinned. Supported by PHS grants GM00260, HL13517, and AM17081.

**TH-PM-B6** LATENCY - RELAXATION OF MUSCLE IS NOT RELATED TO $Ca^{++}$ RELEASE PER SE. A. Gilai*, and G. E. Kirsch*, (intr. by E.J. Peck, Jr.), Dept. of Biol. Sci., Purdue Univ., W. Lafayette, Indiana 47907

Latency relaxation (LR), twitch tension and membrane potential were recorded in single muscle fibers of Xenopus stretched to a length 140% of slack length and stimulated massively (0.05 ms). Tension was measured with a strain-gauge transducer (Pixie 8206, Endevco) with a sensitivity of 33.4 μN/mV. Latent period and the duration of LR were 1.5ms and 2.9 ms respectively and the average amplitude was 55 N/m$^2$. During low frequency repetitive stimulation of the fiber (1 c/sec) three phases of twitch tension were observed: 1) Negative staircase (8% drop in tension). 2) Positive staircase (27% increase in tension). 3) Fatigue (80% drop in tension). Simultaneous recording of LR showed a continuous (non linear) decline in amplitude with average half time of 31 sec. At the peak of staircase, twitch tension reached a maximum but latency relaxation vanished. The application of twitch potentiators, SCN (12 mM) or caffeine (1 mM), increased the twitch amplitude by 15-36% but, LR amplitude decreased by 30-93%. The application of E-C-uncouplers, $D_2O$ or dantrolene $Na^+$, decreased twitch amplitude by 43-89%. At the same time LR amplitude did not change at all. Resting and action potentials were not significantly changed by repetitive stimulation, potentiating drugs or E-C-uncouplers. In accordance with the view that tension generation is proportional to the amount of $Ca^{++}$ released from the SR, the correlation of changes in twitch tension with corresponding changes in LR, suggest that LR is not related to $Ca^{++}$ release per se.

Supported by NIH Grant NS-08601 and Muscular Dystrophy Association.

TH-PM-B7 THE EFFECTS OF CAFFEINE AND IODOACETIC ACID ON THE STRESS-STRAIN BEHAVIOR OF FROG SKELETAL MUSCLE. R.P. Schwarz, Jr.*, R.T. Hsieh, and W.H. Johnson, Dept. of Biology, Rensselaer Polytechnic Inst., Troy, N. Y. 12181

Whole frog sartorius muscle in caffein contracture at 20° C displayed elastic properties similar to those obtained from an iodoacetate-treated rigor preparation. The elastic modulus for a muscle equilibrated for one hour in 5.0 - 10.0 mM caffeine Ringer's solution was 6.7 times greater than that obtained for the same muscle in a caffeine-free medium. Addition of 3.0 mM caffeine increased the elastic modulus by a factor of 4.5 over the control case, while a potentiation-producing caffeine concentration of 1.5 mM produced no change in stiffness. Muscles in IAA rigor exhibited elastic modulus increases of 7.0 times the control case. In addition, the parameter (caffeine twitch tension/normal tetanus tension) was recorded as a function of time after the addition of the drug. It was observed to increase initially and then to diminish steadily, becoming zero coincidental with the appearance of peak contracture tension. The results of our experiments suggest that caffeine at irreversible contracture-producing concentrations somehow induces a rigor or rigor-like state in muscle. (Supported by Muscular Dystrophy Assoc.)

TH-PM-B8 EFFECT OF ADRENALINE ON THE CONTRACTILE PROPERTIES OF THE FROG SKELETAL MUSCLE. R. Valle-Aguilera* and H. González-Serratos, Dept. of Pharmacol. and Dept. of Physiol., Centro de Investigación y de Estudios Avanzados del IPN, México, D.F., México.

The present experiments were undertaken to investigate if adrenaline has some effect on the contractile properties of frog isolated skeletal muscle fibres and to analyse if some of the E-C coupling steps or the contractal material were involved in it. Adrenaline has the following effects on single twitches when compared with the control ones: a) the peak tension increases between 1.1 to 1.8 times when adrenaline concentration varies from $1 \times 10^{-7}$ to $1 \times 10^{-5}$ M, b) the rate of rise of tension development is augmented to approximately 1.51 times with the same concentration; c) the duration from the onset of the twitch to its peak is variable and slightly larger and d) the total duration of the twitch is only slightly increased being therefore the relaxation faster. Adrenaline does not affect maximal tetanic tension, but increases the rate of tension development about 20% with no relationship to the right branch of the length tension curve. The results can be explained assuming that adrenaline increases the amount of $Ca^{++}$ pumped into the SR. Since adrenaline increases the twitch tension under fatigue (1), the results described here are in agreement with the proposition that fatigue is due to a depressed SR $Ca^{++}$ pump (2). (Supported by the Muscular Distrophy Associations of America, Inc.) 1. Brown, Bulbring & Burns. J. Physiol. 107, 115 (1948). 2. H. González-Serratos, L.M. Borrero & C. Franzini-Amstrong. Fed..Proc. 33, 5 (1-74).

TH-PM-B9 INHIBITION OF Ca, SUBSTRATE AND RIGOR-TENSIONS BY ATP. Jenny R. Zollman, Donald S. Wood*, and John P. Reuben, Dept. of Neurology, College of Physicians and Surgeons, Columbia University, New York, N. Y. 10032

Tension development in chemically-skinned rabbit psoas and human skeletal muscle fibers requires MgATP as substrate. ATP, not associated with Mg (abbrev. ATP) when increased stepwise from 0.5 mM to 20 mM, progressively attenuates isometric tensions caused by (1) low concentrations of buffered substrate (.03-100 μM) in the absence of Ca ($< 10^{-9}$ M), (2) saturating levels of Ca ($10^{-4}$ M) at substrate concentrations of 0.5-10 mM, or (3) removal of MgATP (rigor). The shape of the monophasic tension vs substrate curve, obtained in the absence of Ca, is dependent upon the level of ATP in the saline. Curves generated in .5 mM ATP are broader than in 5 mM ATP. At 100 μM substrate, fibers in 0.5 mM ATP are only 15% relaxed from the maximum tension while fibers in 5 mM ATP are 85-100% relaxed. ATP also attenuates maximum Ca tensions ($P_o$) by 5-25% over a large range of substrate concentrations (0.5-20 mM). The effects of ATP on both substrate and Ca tensions are completely reversible. The rigor tensions (3-15% $P_o$) induced by washing the fibers with substrate-free solutions containing 10 EDTA mM are subsequently attenuated (5-100%) by addition of ATP (5-20 mM). Unlike the effects on Ca or substrate tensions, this attenuation cannot be reversed by removal of the ATP. Other nucleotide polyphosphates (5-20 mM) produce little (ITP) or none (ADP) of the relaxing effects that are observed with ATP on these mammalian preparations. Supported in part by H. Houston Merritt Clinical Res. Ct. for Muscular Dystrophy and Related Disease; NINDA and NHLI.

**TH-PM-B10** EQUATORIAL X-RAY REFLECTIONS FROM REST FROG SARTORIUS. R. W. Lymn, National Institute of Arthritis, Metabolism, and Digestive Diseases, NIH, Bethesda, MD 20014

The form factor describing X-ray scattering by the helical packing of myosin into the thick filament is $F_m(R,\psi,1/c) = \sum_n(\sum_j f_j J_n(2\pi r_j R) \chi \exp[i\{n(\psi + \pi/2 - \phi_j) + 2\pi l z_j/c\}]$, where c is the pitch of the helix, l is the layer line number, and n is determined by the selection rules, $l = nt + um$, and $n = gN$. (There are u asymmetric units in t turns of the basic helix, and there are N basic helices, i.e. strands; j indexes subunits.) This can be convoluted with the transform of the hexagonal unit cell, along with similar form factors, $F_A$, for the actin helices, to give the form factor for the equatorial reflections, (Eq. 1) $F(R,\psi,0)_{hk} = F_m \exp(in\theta) + F_A\{\exp i\nu\alpha \exp 2\pi i(h/3 + 2k/3) + \exp i\nu\beta \exp[-2\pi i(h/3+2k/3)]\}$ where h and k are the indexes of the equatorial reflections, θ is the azimuthal angle made with the side of the unit cell by a myosin unit, while α and β are the angles made by actin units in the two thin filaments. ν is determined by the selection rule for actin. Use of equation 1 allows one for the first time to use the same model to calculate axial and equatorial reflections from skeletal muscle. Experimental equatorial measurements of resting frog sartorius can be fit by either three or four stranded molecules in which the myosin cross arm extends to a radius of 200 Å, which is the distance to the trigonal points of the unit cell. This is also consistent with the axial pattern. Further, because of the selection rules, the first non-zero Bessel terms, $J_n$, are either $J_9$ or $J_{12}$. These become appreciable only for reflections higher than 30. Thus the change in relative intensities of the lower orders upon excitation can be due solely to disordering of the myosin helix, caused either by binding to actin or some intrinsic property of the myosin filament.

**TH-PM-B11** X-RAY DIFFRACTION OF SHORTENING SARTORIUS MUSCLE. L. C. Yu,* R. N. St. Onge,*† R. W. Lymn, and R. J. Podolsky, National Institute of Arthritis, Metabolism, and Digestive Diseases, NIH, Bethesda, Maryland 20014, and †Department of Physics, University of New Hampshire 03824.

Equatorial X-ray diffraction patterns from resting and activated sartorius muscles were obtained using an electronic position sensitive detector (PSD) with 100 μm resolution. In conjunction with the PSD, electronic gating was designed to record patterns from different physiological states; (1) resting state before activation, (2) isometric contraction at long sarcomere length, (3) isotonic contraction, (4) isometric contraction at short sarcomere length. The load of shortening ranged between 0.14 and 0.40 of $P_o$. While the ratio of the intensities $I_{10}/I_{11}$ decreased approximately by a factor of five upon activation, it remained essentially the same for both isometric and isotonic contraction. Analysis of the (10) and (11) reflections separately showed that $I_{10}$ and $I_{11}$ both increased by a small, possibly significant, amount in the transition from the isometric to isotonic state. The results show that once the muscle is fully activated, changes in force have much smaller effect on the equatorial reflections than the original transition from rest to activation. If the intensity ratio can be taken as a measure of cross-bridge number, the results provide evidence that the drop in tension in a shortening muscle is due primarily to changes in the force and configuration of the individual cross-bridges rather than the total number.

**TH-PM-B12** THE KINETICS OF CROSS-BRIDGE TURNOVER IN SKINNED MUSCLE FIBERS: EFFECTS OF KCl AND CALCIUM. Jagdish Gulati and Richard J. Podolsky, NIH, Bethesda, Md., 20014

The force developed by the skinned frog fibers can be modulated by both the level of free calcium ions and the ionic strength. Lowering the free calcium concentration has the same effect on both force and velocity as increasing the KCl. In order to study the way in which these agents affect the force, their influence on the isotonic velocity transients was examined. At pCa 5, raising the KCl from 140 to 210 mM decreases the force about two fold. Conversely, lowering the KCl from 140 to 20 mM increases the force two fold. As shown previously (Fed. Proc. 33:1260,1974), the amplitude of the transients is increased in high KCl and is suppressed in low KCl. The null time (J. Physiol. 184:511,1966) at a given relative load was the same in 140 mM and 210 mM KCl. The effect of KCl on the amplitude of the transient indicates that the kinetics of cross-bridge turnover are changed with ionic strength. The effect of changing free calcium from pCa 5 to 6.4, at 140 mM KCl, was studied in six preparations. While the force developed in pCa 6.4 was half that in pCa 5, both the null times and the amplitude of the transients were the same at both calcium levels. The results show that the kinetic properties of the cross bridges are unaffected by these changes in pCa, and they provide additional evidence that calcium affects force by controlling the number of activated cross bridges.

**TH-PM-B13** PRESERVATION OF X-RAY PATTERNS FROM FROG SARTORIUS MUSCLE PREPARED FOR ELECTRON MICROSCOPY. M. K. Reedy, Anatomy Department, Duke University Medical Center, Durham, N.C. 27710.

The helical features of vertebrate actin and myosin filaments are obscured in thin sections. Corresponding layer lines of the low-angle X-ray pattern are lost during conventional specimen preparation. I am trying to preserve the X-ray pattern of resting frog sartorius, in order to obtain thin sections where the helical symmetry of crossbridge arrangement can be visualized directly. Primary fixation by glutaraldehyde best preserves the relaxed pattern. Primary fixation by the di-imido esters, as well as formaldehyde or dilute glutaraldehyde (< 0.5%), convert the pattern (including equatorials) to rigor, so these are not being used. Secondary fixation is aimed at supplementing the amino-directed crosslinks of aldehyde fixation by additional crosslinks. Free aldehydes can be engaged by diamino compounds. Carboxyl groups (outnumbering the lysines 3:1 in myosin and 4:1 in actin) can be activated by carbodiimide treatment and then "converted" to aminos by short-chain diaminos for subsequent treatment with glutaraldehyde, or else crosslinked directly with longer chain diaminos. Hydroxyl and other groups may be engaged with polyfunctional alkylating agents like TAPO or triethylenemelamine. Each of these strategies has preserved actin and myosin layer lines through acetone dehydration, but not through embedding. However, combinations (for example: Glut-TAPO → carbodiimide-ethylenediamene → Glut) have succeeded; actin layer lines and weak myosin layer lines have now been obtained from epoxy-embedded muscles after such treatments. Very preliminary optical analysis of initial EMs has not yet borne out the promise of higher fidelity images.
Supported by NIH and MDAA.

**TH-PM-B14** X-RAY SCATTERING AT SMALL ANGLES BY SOLUTIONS OF SUBFRAGMENT-1 OF MYOSIN. K.M. Kretzschmar*, R.A. Mendelson, and M.F. Morales. CVRI, University of Calif., San Francisco.

An apparatus for the detection of X-radiation scattered at small angles by solutions of macromolecules was designed and constructed for use with the source of synchrotron radiation (wave length=1.48Å) available at the S.S.R.P., Stanford Linear Accelerator Center. The beam was intrinsically highly collimated; it only required to be shaped by a system of slits before it impinged on the sample. Intensity was measured as a function of angle using a sodium iodide detector mounted on a remotely controlled micrometer stage. Results using solutions of bovine serum albumin agreed with published data. Subfragment-1 of myosin (S-1) was prepared according to Lowey and concentrated by precipitation with ammonium sulfate. The preparation was characterized using SDS gel electrophoretograms and measurements of ATPase activity. The X-ray scattering showed no detectable dependence of the apparent radius of gyration on the concentration of S-1 over the range investigated (10mg/ml to 2mg/ml). Thus the radius of gyration of S-1 (the limit of the value of the apparent radius of gyration at zero concentration) was equal to the measured radius of gyration and was about 32Å. If S-1 is assumed to be a prolate ellipsoid of revolution, of uniform electron density and with a molecular weight of $1.15 \times 10^5$, then the axial ratio of this ellipsoid is about 2.8 and the major axis is about 130Å long (excluding any outer shell of water that the molecule might possess). Measurements of fluorescence anisotropy decay (Mendelson et.al., Biochem 12, 2250, 1973) also suggest that S-1 is elongate. (We are indebted to S.S.R.P. Supported by NSF Grant GB 24992-X, USPHS Grants HL-16683 and HL-06285, and the British Science Research Council).

**TH-PM-B15** DOES $Ca^{2+}$ AFFECT ROTATIONAL BROWNIAN MOVEMENT OF S1 MOIETIES IN SYNTHETIC THICK FILAMENTS? R. Mendelson and P. Cheung, CVRI, Univ. of Calif. San Francisco, California.

We have studied the effect of $Ca^{2+}$ on rotary movements of 1,5 IAEDANS labelled S1 moieties of (skeletal) synthetic filaments using time resolved fluorescence depolarization. Different preparations (Harrington, Huxley, Morimoto , and Kaminer) have been studied. In summary, we have found that although filament formation tends to immobilize S1, no statistically significant effect of $Ca^{2+}$ was found in either the presence or absence of $Mg^{2+}$ ATP (or $Mg^{2+}$ AMPPNP). However, S1 mobility increases with increasing pH. Filament order decreases with increasing pH (Kaminer), so mobility and order correlate negatively. If $Ca^{2+}$ makes S1 radiate out from the filament axis, we expect mobility should increase. When pH shifts from 8.3 to 6.8 the shorter (log anisotropy vs. time is biphasic) rotational correlation time, $\phi$, shifts from 500 to 900nsec (80% change). But at pH 6.8, when pCa shifts from approx. 8.5 to 4, the $\phi$ change is small: $(\Delta\phi/\phi)\times100=(2.3\pm3.5)\%$ (s.e.m. 13 difference measurements). Why Morimoto and Harrington (J. Mol.Biol. 88, 1975) observed $Ca^{2+}$ to increase s and decrease $\eta$ is unclear. Results here agree with fibre work (Nihei et.al. PNAS 71, 1974). Since S1 is elongate and swivel-attached (Mendelson et.al. Biochem 12, 1973 and Mendelson et.al. J. Supramol.Struc. 3, 1975) we think S1 reaches actin by translational Brownian motion over a short distance. Rotary freedom of S1 allows it to "roll" on actin during contraction. Restricted mobility of S1 when near the filament core positions it over the new, downstream (if sliding) actin site after rotation. (Supported by USPHS HL 6285, HL 16683 and NSF GB24992-X).

**TH-PM-C1** TWO TIME-CONSTANT ELECTICAL MODEL OF FROG SKIN EVALUATED WITH ISOPROTERENOL AND AMILORIDE. Don W. Watkins, Physiology Department, The George Washington University Medical School, Washington, D.C. 20037

Previous studies on the impedance of frog skin have noted that the data were best explained by either a single, parallel resistance-capacitor (RC) pair (one time-constant) or a polarization element. In this study the alternating current (AC) impedance measurements were directed to comparing the data obtained with characteristics of a two time-constant circuit model. Under control conditions the data were not well fitted by a single RC pair, however the necessity for a second RC pair was not always obvious. Application of amiloride greatly increased the direct current resistance and changed the AC data to give a better fit with one RC pair. Isoproterenol reduced the direct current resistance and altered the AC data so that two RC pairs were needed. These results are compatible with the hypothesis that the electrical impedance of frog skin is due to the sum of the contributions from two membranes, each having its own RC characteristics. The outward-facing membrane has a higher resistance and thus partially dominates the impedance characteristics under control conditions, or completely dominates with amiloride. After isoproterenol, however, the high resistance of the outer membrane is reduced and the time-constant of the inner membrane contributes significantly to the impedance. Supported by: NSF 74-08901

**TH-PM-C2** DIFFUSION OF XENON THROUGH ISOLATED FROG SKIN AND TOAD BLADDER. G.L. Pollack, Physics Department, Michigan State University, East Lansing, Michigan 48824

Xenon and the other rare gases are comparatively inert but yet undergo several interesting interactions with biological systems. An important component of these interactions is the diffusion of rare gas atoms through and absorption by plasma membranes. We have measured the rate of diffusion of Xe through freshly isolated frog skins and toad bladders. The technique is essentially to measure the transfer rate of $Xe^{133}$, dissolved in Ringer's solution, through a membrane separating two chambers filled with Ringer's solution, by using the gamma-ray radioactivity. Preliminary results for the transfer coefficients, d in molar flux per unit concentration difference, at room temperature give values of about $10^{-4}$ cm/sec for abdominal frog skins and toad urinary bladders. For both systems it was observed that the diffusion rate from inside to outside is the same as the rate from outside to inside. We conclude tentatively that the transfer of Xe is by passive transport in these systems and that there may be a common principal barrier to diffusion. The effects on the Xe diffusion of unstirred water layers, as well as edge effects, have also been considered. Applications will be discussed to general anesthesia, fission reactor emission, nuclear medicine, and other related problems.

**TH-PM-C3** RESPONSE OF $CO_2$ EFFLUX TO CHANGES OF Na TRANSPORT IN THE TOAD BLADDER: COMPARISON OF AMILORIDE WITH OTHER AGENTS. R. E. Steele[+], W. E. Walker*, and R. H. Maffly, Stanford University Medical Service, Veterans Administration Hospital, Palo Alto, CA 94304
([+] Present Address: Laboratory of Technical Development, NHLI, Bethesda, MD 20014)

$CO_2$ efflux and Na transport were measured simultaneously in toad bladders (Colombian Bufo marinus) mounted in Ussing-type chambers. Rapid changes in Na transport (measured by short circuit current) were produced by changing of mucosal [Na], varying of transbladder PD, or adding amiloride. Na transport-related $CO_2$ efflux (determined by a rapid conductometric method) changed more slowly than Na transport. A three-compartment model (representing the bladder, bathing solution and measurement device) without back flux has proved adequate to closely fit the $CO_2$ efflux data. Using step changes in $CO_2$ input, time constants ($\tau$) were determined to be 2.4 min for the Ringer bathing solution and 0.2 min for the measurement device. For changes in both [Na] and PD, the $\tau$ for the bladder approximated 4 min (3.7 $\pm$ 1.8(SD) min, n=27 for $\Delta$[Na] and 4.2 $\pm$ 0.2 min, n=4 for $\Delta$PD). A much larger bladder $\tau$, 8.8 $\pm$ 1.8 min (n=13), was found when amiloride was used (4 - 9 $\mu$M in mucosal bath). Addition of $H_2SO_4$ showed that the bladder $\tau$ actually resulted from a pool of dissolved $CO_2$ and $HCO_3^-$. Decrease in the $CO_2$ permeability of the cell membranes could cause the $CO_2$ pool and $\tau$ to increase; however, neither the overall $CO_2$ permeability nor the time course of the $CO_2$ movement through the bladder was measurably changed by amiloride. An increase in bladder pH would increase the $HCO_3^-$ portion of the total $CO_2$ pool. Although amiloride produces no change in $H^+$ transport by toad bladder (Am. J. Physiol. 223: 1338), amiloride might increase bladder pH without affecting $H^+$ transport by altering the membrane potentials of the transporting bladder cells.

TH-PM-C4 DOES SEROSAL SODIUM RECYCLE THROUGH THE ACTIVE TRANSPORT SYSTEM OF TOAD BLADDER? M. Canessa, P. Labarca and A. Leaf, Laboratory of Renal Biophysics, Massachusetts General Hospital, Dept. of Physiology and Medicine, Harvard Medical School, Boston, Mass. 02114.

A range of values have been reported for the ratio of Na transported to $CO_2$ produced or $O_2$ consumed by epithelia when short-circuited. A possible explanation for such variable stoichiometry is that Na from the serosa (S) medium enters the transporting cells passively, but is pumped out at the basolateral surfaces; such "recycling" of SNa would require energy for its extrusion but not contribute to net transepithelial transport (SCC). To test this possibility, (1) Basal and total $CO_2$ production ($JCO_2$) and SCC were measured either with Na Ringer (NaR) bathing both surfaces or Na-free-R on serosa, (2) Amiloride $10^{-5}$M or Na-free mucosal R (MR) were used to stop Na transport and $JCO_2$ was measured with and without Na in SR. The results of (1) show no significant change in the stoichiometric ratio $dJ_{Na}/dJ_{CO_2}$ when Na in SR was replaced by choline or Mg (13.75 $\pm$ 2.2 and 13.45 $\pm$ 2.2, n=12). The results of (2) show that Na-free-SR caused no further fall in basal $CO_2$ production: 2.21 $\pm$ 0.64 nmoles/mgdw/min, n=7 initially and 2.02 $\pm$ 0.56 after replacement of SNa by choline and 1.34 $\pm$ 0.34 initially and 1.10 $\pm$ 0.2, n=10 after Mg-SR. Similarly, addition of $10^{-3}$M ouabain failed to reduce $J_{CO_2}$ when SCC had been prevented previously by amiloride or choline MR; $J_{CO_2}$ = 2.88 $\pm$ 0.43 nmoles/mgdw/min, n=6 and after ouabain 3.0 $\pm$ 0.46. This experiment indicates that active Na transport not involved in transepithelial transport is negligible. We conclude that "recycling" of SNa must be minimal and cannot account for observed variations in $dJ_{Na}/dJ_{CO_2}$ in toad bladder.

TH-PM-C5 FLUORESCENCE SPECTROSCOPIC STUDIES OF THE FLUIDITY OF TOAD BLADDER CELL MEMBRANES. B.R. Masters, D.D. Fanestil*, and J. Yguerabide, Dept. of Medicine and Biology, University of California San Diego, La Jolla, California 92093.

It has been suggested that the increase in water permeability across intact toad bladder stimulated by vasopressin is mediated through an increase in fluidity of the apical membrane of the granular cell. To test this hypothesis we have initiated studies on the fluidity of the apical membrane using the technique of polarized fluorescence spectroscopy. Studies have been performed on both intact toad bladder and on isolated mucosal cells. Techniques for overcoming the problems of labelling and measuring polarized fluorescence from intact tissue will be discussed. These techniques include phase and fluorescent microscopy to determine the cellular location of the fluorescent label as well as to establish cellular integrety. The results indicate that isolated mucosal cells from the toad bladder labelled with perylene show no change in membrane fluidity upon the addition of either vasopressin or dibutyryl cyclic AMP, but a small decrease in fluorescence polarization of perylene fluorescence is observed in the intact toad bladder. This effect obtained with the intact toad bladder is consistent with our hypothesis that vasopressin increases water permeability by causing an increase in the membrane fluidity.

This work is supported in part by USPHS EY 01177-03 (J.Y.) and AM-14915 (D.D.F.)

TH-PM-C6 TRANSPORT PROPERTIES OF HOG GASTRIC FUNDIC MEMBRANES. G. Sachs, G. Saccomani*, R. Schackmann*, E. Rabon* and H. Hung*. University of Alabama in Birmingham, Laboratory of Membrane Biology, Birmingham, Alabama 35294.

Hog gastric fundic homogenates were purified by differential and zonal density gradient centrifugation, producing 2 membrane peaks. When the denser of these 2 peaks was further separated on free flow electrophoresis using 8 mM buffer with MgATP several peaks were found, the peak closest to the anode being over 40 fold enriched in $K^+$ ATPase, showing a high level of valinomycin stimulation of the enzyme and being the only peak capable of $H^+$ uptake in the presence of ATP. 4 vectorial properties were studied, $Rb^+$ efflux, $H^+$ uptake, ATP enhancement of ANS fluorescence and $K^+$ gradient dependent binding of $^{32}Pi$. At pH 6.1, $Rb^+$ and $H^+$ movement and ANS fluorescence showed an identical time course, and similar cationic dependence and selectivity, and the $K_M$ for $H^+$ uptake, $Rb^+$ efflux and $K^+$ ATPase are the same whereas the $K_M$ for ANS fluorescence is one tenth of those. At pH 7.4 although a pH gradient is developed as measured by $^{14}C$ imidazole redistribution, the major vectorial reactions are $Rb^+$ efflux and an inward $K^+$ gradient dependent protein phosphorylation (NIH, NSF support).

**TH-PM-C7** $Ba^{2+}$ INHIBITION OF "NON-ACIDIC" $Cl^-$ SECRETION BY PIGLET GASTRIC MUCOSA. T. E. Machen and J. G. Forte. Physiological Lab., Downing St., Cambridge, England, and Dept. of Physiology-Anatomy, Univ. of Calif., Berkeley, Ca. 94720.

The effect of 0.5 mM $Ba^{2+}$ on secretory function of histamine-stimulated piglet gastric mucosa was assessed in vitro by measuring transepithelial potential difference (p.d.), resistance (R), $H^+$ secretion, and unidirectional fluxes of $Cl^-$-36 ($J^{Cl}$, in $\mu eq/cm^2 . hr$) during short circuit current ($I_{sc}$) conditions. Mucosal solution = m; serosal = s. R and p.d. were sometimes used to calculate current, $I_{calc}$, generated by the tissue. During control conditions, $Ba^{2+}$ added to the s solution caused p.d. to decrease (33.2 to 18.2 mV) and R to increase (71 to 94 $\Omega . cm^2$). $I_{calc}$ decreased by 45%, but $H^+$ secretion remained constant at 11 $\mu eq/cm^2 . hr$. During $I_{sc}$, $Ba^{2+}$ caused $J^{Cl}_{ms}$ to decrease from 28.0 to 23.2 while $J^{Cl}_{ms}$ increased from 14.5 to 15.8. $I_{sc}$ decreased from 10.2 to 7.6 $\mu eq/cm^2 . hr$. Neither blocking $Na^+$ transport with amiloride nor varying $[Cl^-]$ in the m and s solutions (replaced with gluconate) between 130 and 2.6 mM altered the inhibitory effect of $Ba^{2+}$ on $I_{calc}$. However, as $[K^+]_s$ was increased, this inhibitory effect was depressed, e.g. at $[K^+]_s$=2 mM, 0.1 mM $Ba^{2+}$ caused $I_{calc}$ to decrease by 40%, while at $[K^+]_s$=15 mM, 0.1 mM $Ba^{2+}$ caused $I_{calc}$ to decrease by only 12%. 15 mM $K^+$ itself caused $I_{calc}$ to decrease by 15%. We conclude that $Ba^{2+}$ specifically inhibits "non-acidic" $Cl^-$ secretion for neither $Na^+$ nor $H^+$ transport were affected. The "non-acidic" $Cl^-$ secretion seems to be entirely independent of the HCl secretion process. Also, $Ba^{2+}$ exerts its effect only indirectly by interacting with $K^+$ permeation sites at the s side of the epithelium. The inhibitory effects of $Ba^{2+}$ and high $[K^+]_s$ have also been observed in frog gastric mucosa and thus do not seem to be a peculiarity of the mammalian preparation.

**TH-PM-C8** SIGNIFICANCE OF RETURN IONIC PATHWAYS OF THE SECRETORY MEMBRANE OF FROG GASTRIC MUCOSA IN $Cl^-$-FREE MEDIA. T. L. Holloman,* M. Schwartz, M. A. Dinno,* and G. Carrasquer, Departments of Applied Mathematics, Physics and Medicine, University of Louisville, Louisville, Ky. 40208.

As a result of our studies on inhibitors of $H^+$ secretion in the frog (Rana pipiens) gastric mucosa in $SO_4^{2-}$ media, it has become necessary to study the relative resistances of various ionic pathways. For this purpose, experiments measuring transmembrane resistance, transmembrane PD and $H^+$ secretory rate were done in vitro with $MgSO_4$, $Na_2SO_4$, $K_2SO_4$ singly or with combinations of these salts bathing the secretory side of the mucosa. The $SO_4^{2-}$ Ringer solution on the nutrient side was the same in all experiments. Both sides of the mucosa were gassed with a mixture of 95% $O_2$ and 5% $CO_2$. The pH of the secretory side was maintained at 5.03. The PD with 52 mM $K_2SO_4$ was oriented with the nutrient side positive relative to the secretory side whereas the PD with 52 mM $Na_2SO_4$ or 52 mM $MgSO_4$ was oriented with the nutrient side negative. The resistance with 52 mM $K_2SO_4$ was about 130 ohm $cm^2$ smaller than with 52 mM $Na_2SO_4$ whereas the resistance with 52 mM $MgSO_4$ was about 190 ohm $cm^2$ greater than with 52 mM $Na_2SO_4$. The $H^+$ rate correspondingly was about 0.45 $\mu eq\ hr^{-1}cm^{-2}$ higher for 52 mM $K_2SO_4$ compared to 52 mM $Na_2SO_4$ and about 0.45 $\mu eq\ hr^{-1}cm^{-2}$ lower for 52 mM $MgSO_4$ compared to 52 mM $Na_2SO_4$. It appears that in the absence of $Cl^-$ the cationic pathways become significant as the return pathways of $H^+$ secretion, the $K^+$ pathway providing lower resistance than the $Na^+$ pathway. If $Mg^+$ penetrates into the mucosa, the resistance of its pathway is greater than either of the other two cationic pathways.

**TH-PM-C9** KREBS CYCLE AND H+ SECRETION IN AMPHIBIAN GASTRIC MUCOSA. J.Chacín, R.Rincón*, D.Inciarte*, and A.Cañizales*. Department of Physiology, Zulia University School of Medicine, Maracaibo, Venezuela.

In order to evaluate the contribution of the oxidations of Krebs cycle as energy sources for H+ secretion, the effects of some inhibitors and intermediates of the cycle were investigated using in vitro gastric mucosa of Bufo marinus. Malonate 10mM, and inhibitor of succinate oxidation, significantly ($P < 0.01$) reduced the oxygen uptake (qO2) and the 14CO2 production from 1-14C-succinate. Malonate also inhibited H+ secretion (qH+) by 15% (N=12, $P < 0.05$). Arsenite, an inhibitor of the oxidation of $\alpha$-ketoglutarate, produced a more drastic inhibition on qO2 and 14CO2 production from 1,4-14C-ketoglutarate. Doses of arsenite of 0.5,1,2 and 10mM inhibited qH+ by 23%, 40%,59% and 94% respectively. The effect of arsenite was reverted by washing and addition of lipoate 1mM. Citrate, $\alpha$-ketoglutarate, succinate and malate had no significant effects on qH+ and qO2 at pH 7.4. It seemed that these negative results were due to poor penetration of the intermediates into the cells because the 14CO2 production was significantly higher at pH 5.0, succinate stimulated qO2 at pH 5.0, and succinate increased qO2 by 69% at pH 7.4 when the membrane barrier was eliminated. At pH 5.0, citrate, $\alpha$-ketoglutarate and succinate significantly increased qH+ ($P < 0.005$) by 24%,20% and 22% respectively. These results indicate that the citric acid cycle is an important metabolic energy source for qH+ in toad gastric mucosa. Supported by CONDES of LUZ and Grant S1-0455 from CONICIT, Venezuela.

**TH-PM-C10** THE SUDDEN POTENTIAL DROP IN FROG GASTRIC MUCOSA: EFFECTS OF SUBSTRATE DEPRIVATION. George W. Kidder III, Dept of Physiology, Univ. of Maryland Sch. of Dentistry, Baltimore, Md. 21201

The sudden potential drop (SPD) is a rapid (<1 min) and substantial (10-20 mV) fall in PD across the chambered mucosa which we found to occur regularly when the serosal pH was less than 7.1 and oxygen was excluded (or $CN^-$ added) to stop electron flow in the cytochrome system. Recent experiments show a similar result at pH 6.9 in the presence of $O_2$ if endogenous substrate can be exausted. Using a combination of *in vivo* perfusion and *in vitro* incubation, a "resting" preparation can be obtained in 3 hours, with zero secretory rate, a PD a few mV negative (reversed) and the cytochromes oxidized. Addition of histamine has no effect. Subsequent addition of β-OH-butyrate (βOHB, 10 mM, serosal) causes a prompt (~3 min) partial reduction of cytochrome b with no change in cytochrome c, followed by a sudden rise in PD to normal values (~10 min), with acid secretion and the concomitant reduction of cytochrome c and a further reduction in b occurring much later (30-50 min). Addition of ATP (10-20 mM, serosal) to the resting, aerobic, post-SPD preparation causes minor changes in PD, but does not return PD to normal values nor restore secretion. Subsequent addition of histamine and βOHB (in the presence of ATP) fails to elicit the usual effect, although the tissue can partially recover if the ATP is washed out. Thus, as previously reported for the anaerobic system, exogenous ATP does have marked effects on the tissue, but cannot support acid secretion. The inhibitory effect of ATP remains to be explained. (Sup. by NSF GB-36278)

**TH-PM-C11** CURRENT-VOLTAGE RELATIONSHIP OF ISOLATED RENAL CORTICAL COLLECTING TUBULES: CORRELATIONS WITH ACTIVE Na AND K TRANSPORT. Roger G. O'Neil and Sandy I. Helman, Dept. of Physiology and Biophysics, University of Illinois, Urbana, Illinois 61801.

The I-V relationships of isolated perfused rabbit tubules were determined by injecting pulses of constant current (200 msec) between tubular lumen and the peritubular bath, and recording the resulting transepithelial voltages, $V_T$ (lumen = 0 mV). When the corresponding values of current and voltage were plotted, the data points could be divided into 3 regions of apparent linear resistance, R', R'' and R'''. The voltages at the intersections of the best fit linear regression lines were labelled $E_1$ and $E_3$. From previous observations of others (J. Clin. Invest. 49:1815, 1970; AJP 227:453, 1974), estimates were obtained for the active transepithelial driving forces, $E_{Na}$ and $E_K$, thought to be responsible for active Na reabsorption and active K secretion by the collecting tubule. These literature values of $E_{Na}$ and $E_K$ were similar to the values of $E_1$ (125.6 ± 6.27 mV) and $E_3$ (-43.4 ± 5.23 mV), respectively. With a simple equivalent circuit of the I-V relationship, the currents through the $E_1$ and $E_3$ pathways were calculated and found to average 734 and -158 $pEqsec^{-1}cm^{-2}$, respectively. When these values were compared with the chemically measured rates of net Na reabsorption and K secretion, they were found to be similar, averaging 625 and -174 $pEqsec^{-1}cm^{-2}$, respectively. Thus, it may be that the values of $E_1$ and $E_3$ provide direct estimates of the active driving forces for transepithelial Na and K transport of the isolated cortical collecting tubule.

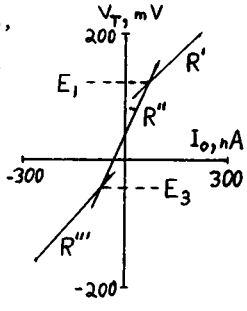


(Supported by Research Grant USPH AM 16663)

**TH-PM-C12** HYDROLASE RELATED GLUCOSE TRANSPORT IN INTESTINAL BRUSH BORDER MEMBRANE VESICLES. R. K. Crane, K. Ramaswamy*, and P. Malathi,* CMDNJ-Rutgers Medical School, Department of Physiology, Piscataway, N.J. 08854.

A vectorial function termed kinetic advantage was ascribed to intestinal brush border membrane sucrase when analysis of early work in this laboratory showed that the products of sucrose hydrolysis were more readily transferred into the cell than glucose released from glucose-1-phosphate (G-1-P) by the action of membrane-bound alkaline phosphatase. More recently (Crane *et al.* Fed. Proc. 29(1970)1952) this vectorial function has been shown to be in fact a sugar transport system distinct from the Na-dependent free glucose transport system. It has been termed Hydrolase Related Transport (HRT). HRT differs from Na-dependent free glucose transport in not requiring sodium, in not being available to free glucose and in being dependent on the action of membrane glycosidases (Malathi *et al.* Biochim.Biophys. Acta 307(1973)613; Ramaswamy, *et al.*, Biochim.Biophys.Acta 345(1974)39). We have further characterized this phenomenon using guinea pig membrane vesicles that are osmotically responsive and exhibit specific characteristics of Na-dependent transport. We proceeded as follows: Intravesicular accumulation was measured using [$^{14}$C]sucrose-([U-$^{14}$C]glucose). From a Na-free medium containing 10 mM [$^{14}$C] sucrose, 800 pmoles of glucose/mg protein were transferred into the vesicles at the end of 1 min incubation. Because free glucose can diffuse into the vesicles the possible diffusion component from any externally released products of sucrase action was measured using [$^{14}$C] G-1-P as a substrate since alkaline phosphatase releases glucose at the membrane surface but does not contribute to HRT. At comparable hydrolytic rates, glucose uptake from G-1-P was only 212 pmoles/mg protein. These results confirm the vectorial function observed in the early work with intact tissue and appear to establish HRT as a membrane transport phenomenon.

**TH-PM-C13** ELECTRICAL CIRCUIT ANALYSIS OF TIGHT EPITHELIA BY ALTERNATING CURRENT TECHNIQUES. C.Clausen*, S.A. Lewis*, J.M. Diamond and R.S. Eisenberg, Department of Physiology, UCLA School of Medicine, Los Angeles, Calif. 90024

Epithelia may be represented by equivalent circuits of resistors and capacitors. An infinite variety of such circuits may be indistinguishable by steady-state DC measurements but distinguishable by AC measurements. Therefore, we used transepithelial AC measurements, combined with intracellular DC measurements, to determine the equivalent circuit and values of the linear circuit parameters for some tight epithelia (rabbit urinary bladder and frog skin). The epithelium is represented by two parallel RC elements (the apical and basolateral membranes) in parallel with a large resistor (the cell junctions) and in series with a small resistor (bathing solution and intracellular fluid). The tissue is mounted by a technique that avoids edge damage. An intracellular microelectrode measures the ratio of the apical to basolateral membrane resistance during transepithelial DC current passage. Transepithelial electrodes measure phase angle and magnitude of the voltage response as a function of current frequency during transepithelial AC current passage. Values of membrane conductances and capacitances are extracted by curve-fitting of the equivalent circuit model to the data. The resulting capacitance values make it possible to normalize membrane conductances to actual surface area of each membrane, and to study tissue conformational changes as a function of stretch and transport rate. (Supported by grants from the NIH).

**TH-PM-C14** INFLUENCE OF $AG^+$ ON EPITHELIAL TRANSPORT. S.D. Klyce, Division of Ophthalmology, Stanford Medical Center, Stanford, Calif. 94305

To establish reversible metal/electrolyte junctions with low contact resistance, current sending Ag/AgCl halfcells are often placed directly in solutions bathing biomembranes. However, trace amounts of $Ag^+$ can modify the function of some epithelia.

Despite the fact that the concentration of ionized Ag in the presence of .1M $Cl^-$ should be less than $10^{-11}$M, cathodal current delivered with a Ag/AgCl halfcell to the tear (mucosal) side of the isolated rabbit cornea can increase corneal epithelial short circuit current (SCC), potential (PD), and conductance (G). These effects are abolished by replacing tear side $Na^+$ with TRIS but are relatively independent of $Cl^-$ concentration.

Using agar Ringer bridges to separate halfcells from bathing media, cathodal current does not stimulate transport, but addition of $10^{-5}$M $AgNO_3$ to the tear side increases absorptive $Na^+$ transport from 0.030±0.009 μEq/cm hr to 1.27±0.20 μEq/cm hr, a steady value sustained for 3 hr. Increased SCC is reversed by reducing agents and is inhibited by pretreatment with ouabain ($ID_{50}$ = 2-6 x $10^{-7}$M). The locus of the primary effect is probably the outer membrane of the surface cell, since the membrane PD is strongly depolarized by $Ag^+$ and since epithelial mannitol permeability is only slowly increased. SCC, PD, and G of the isolated rabbit urinary bladder are also increased by $Ag^+$ ($10^{-5}$M) when the tissue is transporting $Na^+$ at a low rate.

The findings suggest that the primary effect of $Ag^+$ on these high resistance epithelia is an increase in outer membrane $g_{Na}$, which in turn stimulates absorptive $Na^+$ transport. Furthermore, the effect seems to occur primarily via the transcellular pathway.

Supported by USPHS Research Grant EY 00915 from the National Eye Institute.

**TH-PM-C15** ANION PERMEABILITY OF NONEDGE-DAMAGED FROG SKIN., D.D. Macchia and S.I. Helman. Dept. of Physiology and Biophysics, Univ. of Illinois, Urbana, Illinois 61801.

Studies were done to determine the permeability (P) of the isolated skin to $Cl^-$ and $SO_4^=$, and from this to estimate the possible contribution of these anions to the conductance of the shunt pathway. In control skins, continuously short-circuited, permeability to $Cl^-$ was 1.25 ± .36 x $10^{-7}$ cm/sec (N=8) and permeability to $SO_4^=$ was much lower, 0.18 ± .04 x $10^{-7}$ cm/sec (N=7), for skins bathed with chloride- and sulfate-Ringer, respectively. The partial resistances of $Cl^-$ and $SO_4^=$ calculated from the values of P and their concentrations in solution were 22,835 ± 5,189 and 151,193 ± 58,543 Ωcm$^2$, respectively. When these values were compared with the values of shunt resistance, $R_S$, determined by other methods (~7000 Ωcm$^2$, Yonath and Civan, $E_1I_1$), it was apparent that the partial resistances calculated from the passive transepithelial fluxes of $Cl^-$, $SO_4^=$ and $Na^+$ could not account for the values of the shunt resistance ($r_{Na}$ estimated previously to be >500,000 Ωcm$^2$). Accordingly, it is possible that the $R_S$ determined electrically may include transcellular pathways consisting of a series of membranes of different ionic permeability that do not permit transepithelial isotopic fluxes but these membranes could contribute to the electrically determined conductance. If this view is tenable, it would not be surprising to observe that $R_S$ determined electrically was less in value than the values of $R_S$ estimated from the partial conductances determined isotopically. (Supported by Research Grant USPH AM 16663.)

**TH-PM-D1** STABILITY OF AN IN VITRO PHOTOCHEMICAL SYSTEM FOR $H_2$ EVOLUTION. L. Packer, I. Fry*, S. Sarma* and K. Rao*, Univerisity of California, Berkeley, Calif. 94720, and University of London King's College, London, England.

In 1961, Arnon (Science 134, 1425), reported $H_2$ evolution from photosystem I in illuminated chloroplasts supplemented with bacterial ferredoxin and hydrogenase. Recently, this system was shown to work, in principle, with $H_2O$ as the electron donor (Benemann, et al., 1973, PNAS 70, 2317; D.O. Hall, 1975 FEBS Letters, in press). We are characterizing factors upon which such a system in vitro depends, and are evaluating stability of the reaction sequence components. At 15°C light-dependent $H_2$ evolution occurs continuously for 24 hr with either photosystems II and/or I as electron donors. The coupled system is $O_2$ sensitive as previously reported. The relative order of stability of the reaction component was: hydrogenase > photosystem I/II. The presence of bovine serum albumin apparently acting as a fatty acid scavenger affords additional stability (Takaoki, et al., 1974, BBA 352, 260). $H_2$ evolution is about 20 μmoles/mg Chl/hr calculated for initial rates.

During experiments at 15°C a dark hydrogenase activity develops after 30 hr. Dark $H_2$ evolution (sensitive to streptomycin and penicillin) was traced to an organism apparently present in chloroplasts. This is contrary to a dark activation of algal chloroplast hydrogenases recently reported by Ben Amotz et al., 1975, Plant Physiol. 56, 7277; this is being further characterized. (Supported by ERDA and NATO)

**TH-PM-D2** OSMOTIC BEHAVIOR OF MITOCHONDRIAL GHOSTS. Charles Bowman*, Henry Tedeschi, Beth DiDomenico*, and Fred Tung* (Intr. by Sally Izzard), Dept. of Biological Sciences, State University of New York at Albany, Albany, N.Y. 12222.

Experiments were carried out with water treated rat liver mitochondria (mitochondrial ghosts) previously studied by Caplan and Greenawalt [J. Cell Biol. 39, 661 (1968)]. Despite a loss of over half of the total protein and most of the internal cations, the ghosts were found to exhibit osmotic behavior in sucrose solutions. The permeability to nonelectrolytes was found to be similar to intact mitochondria except for a high permeability to ($^{14}C$) sucrose when suspended in sucrose solutions. At least at higher concentrations of sucrose (e.g. 0.3 osmolal) the space permeable to ($^{14}C$) carboxydextran increases. This increase is consistent with the explanation that invaginations in the membranes occurred. In fact, under these conditions cristae-like invaginations could be observed with the electron microscope. Aided by a grant from the American Cancer Society, Inc., BC-161.

**TH-PM-D3** ULTRASTRUCTURAL CONSIDERATIONS IN REGULATION OF MITOCHONDRIAL OXIDATIONS. P. V. Blair and E. A. Munn*, Indiana University School of Medicine, Indianapolis, IN. 46202, and Institute of Animal Physiology, ARC, Babraham, Cambridge, England.

An optimal uncoupling level of dinitrophenol (DNP) induced maximal succinate oxidation only during dynamic contraction of rat liver mitochondria incubated in isosmotic sucrose-phosphate neutralized with $Na^+$, $K^+$, or $Li^+$ (pH 7.2). Attainment of maximal contraction produced over a 50% decrease in uncoupled oxidation rates. High concentrations of DNP (1 mM) inhibited uncoupled succinate oxidation less than 30% during dynamic contraction, but an additional 40-50% inhibition of succinate oxidation ensued upon approaching maximal contraction. Partial mitochondrial swelling, initiated by phosphate or other permeant anions (arsenate and acetate), is necessary for the subsequent inhibition of oxidation rates which occur at maximal contraction induced by DNP. Rates of mitochondrial contraction increased as both phosphate and DNP concentrations were increased. The concomitant attainment of maximal contraction and inhibition of succinate oxidation by 100 μM DNP was reversed by bovine serum albumin (BSA). Following this reversal the mitochondria responded normally to adenosine diphosphate (ADP), oligomycin, anaerobiosis, aerobiosis, and additional DNP (500 μM). Electron micrographs revealed that the inner membrane-matrices of the mitochondria were expanded before addition of DNP, partially contracted after addition of 40 μM DNP, maximally contracted after addition of 80 μM DNP, reexpanded after addition of 100 mg BSA (25 mg/ml), recontracted after addition of ADP, and reexpanded again after addition of oligomycin. These results indicate a possible role for ultrastructural changes in the inner membrane-matrix as a means for regulation of mitochondrial succinate oxidation and by extrapolation to overall intramitochondrial metabolism. (Supported by Grants from USPHS, NIH (AM13939 & GM52221) and the Grace M. Showalter Residuary Trust.)

**TH-PM-D4** MITOCHONDRIAL TRANSPORT OF GLUTAMATE STUDIED BY ISOTOPE EXCHANGE AT EQUILIBRIUM. W. Lebing* and C.M. Smith, Dept. of Biochemistry, Temple University Medical School, Phila., Pa. 19140.

Rat liver mitochondria (respiratory control ratios of 7 to 12) were equilibrated at 22°C with various concentrations of L-glutamate (G) in iso-osmotic medium containing 25μM rotenone and 1000μM arsenite to inhibit glutamate metabolism. A constant amount of $^{14}$C-L-glutamate was added to the incubation mixture and after time intervals of 3.5 sec to 10 min the mitochondria spun through silicone oil into PCA. Rate of glutamate exchange (R) was calculated from the fraction of isotopic equilibrium attained at given times and final matrix G. Matrix and intermembrane volumes were determined with $^{3}H_2O$ and $^{14}$C-sucrose. Plots of the fraction of isotopic equilibrium reached vs time were identical for 0.625mM < G < 10mM. The data when plotted as R vs G fell on straight lines and did not show saturation kinetics. In 9 experiments measured values of 1/R ranged from 38.4 to .84 (R in nmoles/sec-mg); 1/G ranged from 1.6 to .1 (G in mM). The plots of 1/R vs 1/G fitted to straight lines by least squares intersected the axes at 1/R = 0.44 ± 1.276 and 1/G = .0335 ± .0702, close to the intersection of (0,0) predicted by a restricted diffusion mechanism. The exchange of $^{14}$C-D-glutamate was as rapid as that of $^{14}$C-L-glutamate and both stereoisomers reached concentration gradients of approx 2:1 (matrix:medium). N-ethylmaleimide, a weak inhibitor of the glutamate -OH transport system (Meijer, et al. Biochim Biophys Acta, 1972), inhibited exchange of both the D and L isomers. The lack of stereospecificity and the linear relation between exchange rate and glutamate concentration indicates that glutamate translocation in rat liver mitochondria does not require tight binding to a carrier molecule. (Supp. by USPHS grant AM 18045 and grant # IN-886 from the Am. Cancer Soc.)

**TH-PM-D5** DOES A TRANSITION STATE GIVE RISE TO AN INTERMEDIATE MITOCHONDRIAL PHOSPHATE-WATER EXCHANGE CHARACTERIZED BY RESISTANCE TO UNCOUPLERS? R. A. Mitchell, C. M. Lamos,* and J. A. Russo,* Department of Biochemistry, Wayne State University School of Medicine, Detroit, Mi, 48201.

Submitochondrial heart particles catalyze a Pi ⇄ $H_2O$ oxygen exchange accompanying ATP hydrolysis. In the presence of an ATP-regenerating system the exchange is small (about 30% more oxygen from $H_2O$ is incorporated into Pi than would be expected for simple hydrolysis, but this residual exchange is not decreased by 20 mM arsenate (Asi) or 0.5 mM 2,4-dinitrophenol (Mitchell et al., 170th ACS National Meeting, BIOL 107, 1975). These experiments used [ATP] > $K_m$ (apparent) for ATP hydrolysis. If [ATP] < $K_m$ (apparent) there is an increase in exchange (up to approximately 1 extra oxygen/Pi), by a process which is inhibited by oligomycin but not by Asi or dinitrophenol. This exchange seems to represent an intrinsic feature of the catalytic process and may represent the presence of a pentacovalent phosphorus intermediate capable of stabilization by pseudorotation (Westheimer, Accounts. Chem. Res., 1, 70, 1968). Destabilization of ATP relative to the transition state could be accomplished by enzyme-induced strain, so that ATP would resemble a strained phosphodiester (Jencks, Brookhaven Symposia in Biology, No. 15, 134, 1962).

Supported by N. I. H. grant GM 19562 and grants-in-aid from the Michigan Heart Association and from Wayne State University.

**TH-PM-D6** THE ROLE OF THE MITOCHONDRIAL UNCOUPLER BINDING SITE IN UNCOUPLING OF OXIDATIVE PHOSPHORYLATION. W. G. Hanstein, Department of Biochemistry, Scripps Clinic and Research Foundation, La Jolla, California 92037

Equilibrium binding of uncouplers by mitochondria and submitochondrial particles involves unspecific partitioning and interaction with a specific uncoupler binding site characterized by dissociation constants $K_D$ and other parameters. For uncouplers such as azide, 2,4-dinitrophenol, 2-azido-4-nitrophenol (NPA), pentachlorophenol, trinitrophenol and S-13, there is a good correlation (r = 0.99) between $K_D$ and the concentration necessary for 50% uncoupling ($\phi_{\frac{1}{2}}$): $\phi_{\frac{1}{2}}/K_D \approx 0.4$ at 30°C. A simple kinetic model of uncoupling based on stoichiometric uncoupler binding can account for these data. The steady state rate in the reaction cycle $A \xrightarrow{k_1} B \xrightarrow{k_2} C \xrightarrow{k_3} A$ is $k_1k_2k_3/(k_1k_2 + k_1k_3 + k_2k_3)$ at A + B + C = 1. $k_1$ is a function of the uncoupler concentration U, $k_1 = k_o + k_u \cdot U/(U + K_D)$. A is a high energy state, and B and C are low energy states of the same carrier in the electron transport system. A and B are reduced, and C is oxidized (or vice versa). The deenergization step A⟶B is assumed to be rate limiting in the absence of uncouplers ($k_1 = k_o \ll k_2, k_3$). With all rates about equal in the uncoupled state ($k_o:k_2:k_3:k_u$ = 1:100:100:100), a value of $\phi_{\frac{1}{2}}/K_D$ = 0.34 and a respiratory control ratio (RCR) of 34 are calculated. Higher values of $k_u$ result in lower $\phi_{\frac{1}{2}}/K_D$ values and higher RCR's. A binding site able to interact with both small (azide) and large (S-13) uncouplers is likely to be limiting in one or two dimensions only. It may therefore have the shape of a cleft, either in a single polypeptide, or as part of the contact interface between two adjacent proteins. Photoaffinity labeling studies with NPA suggest the latter possibility with the involvement of an uncoupler binding protein (MW 31,000) and subunit 1 of $F_1$-ATP'ase. (Supported by USPHS grant GM 19734).

**TH-PM-D7** KINETICS OF ATP DEPENDENT $Mg^{2+}$ FLUX IN ISOLATED MITOCHONDRIA. E. Kun Dept. Pharmacology, (Surge 103) Biochemistry & Biophysics and the Cardiovascular Research Institute, University of California-San Francisco, San Francisco, CA 94143.

Kinetics of influx and efflux of $Mg^{2+}$ from the mitoplast compartment of mitochondria was followed by a low temperature rapid filtration technique. $Mg^{2+}$ flux in conventionally prepared mitochondria is modified by metabolites of the biosynthetic pathway of glucoproteins, but these effects are eliminated when lysosomes are removed by treatment with low concentration of digitonin. Mitochondria freed from lysosomes perform oxidative phosphorylation at 30° for at least an hour at a rate of 300 n moles ATP/mg protein per minute, whereas this rate is 100 n moles/mg per minute in conventionally prepared particles with a $t_{1/2}$ = 6-10 minutes. The rate of $Mg^{2+}$ uptake in lysosome free mitochondria depends on the concentration of externally added $Mg^{2+}$ (approx. Km = 12 mM), requires ATP and is independent of phosphorylative respiration. Endogenous or added reducing substrates enhance ATP dependent $Mg^{2+}$ uptake, despite 95% inhibition of respiration by oligomycin. Kinetic parameters were determined from the study of time course of $Mg^{2+}$ flux and rate equations were derived which describe the bi-directional flux of $Mg^{2+}$. Ruthenium red inhibits $Mg^{2+}$ flux and uncouplers reverse its direction.

**TH-PM-D8** BINDING OF FLUORESCENT LANTHANIDES TO MITOCHONDRIAL MEMBRANES AND CA (II) BINDING PROTEINS, R. B. Mikkelsen* and D. F. H. Wallach, Radiobiology division, Tufts New England Medical Center, Boston, Mass. 02111. Supported by NSF, American Cancer Society(DFHW) and Damon Runyon Memorial Fund (RBM).

Binding of terbium to rat liver mitochondria ( < 30µg protein/ml) enhances the $Tb^{3+}$ ion fluorescence at 545 nm ∿ 1000-fold and shifts its excitation maximum from 352nm to 285nm. At the low membrane levels used, inner filter effects are not significant and the fluorescence changes indicate the presence of aromatic amino acids near the $Tb^{3+}$ binding site(s). Subfractionation of the mitochondria and use of nonpermeant chelating agents localize $Tb^{3+}$ binding to the outer surface of the inner membrane. At neutral pH, binding is not altered by inhibitors of respiration or oxidative phosphorylation. Soluble mitochondrial $Ca^{2+}$-binding protein (Lehninger (1971) Biochem. Biophys. Res. Commun. 42, 312) also binds $Tb^{3+}$ with a ∿ 1000-fold fluorescence enhancement. Quenching studies with other lanthanides indicate more than one binding site/protein molecule. Binding is not affected by treatment with neuraminidase or $CHCl_3/CH_3OH$ extraction. pH titrations show involvement in $Tb^{3+}$ binding of groups with pK ∿ 6.0. At pH > 7.5 the amount of $Tb^{3+}$ bound to $Ca^{2+}$-binding protein decreases, but the opposite occurs with intact mitochondria. The large fluorescence enhancement seen with intact mitochondria at elevated pH is blocked by antimycin A and rotenone.

Similar $Tb^{3+}$ titration studies comparing mitochondria from normal and SV40-transformed lymphocytes show 2-3-fold greater fluorescence enhancement in the latter. This supports the suggestion that mitochondrial calcium metabolism may be altered in neoplastic cells. (R. F. W. Thorne and F. L.Bygrave (1973) Biochem. Biophys. Res. Commun. 50, 294).

**TH-PM-D9** COUPLING OF RESPIRATION AND PROPERTIES OF VESICLES FORMED WITH SOYBEAN PHOSPHOLIPIDS AND CYTOCHROME *c* OXIDASE FROM YEAST. A. Peña* and H.R. Mahler, Mitochondrial Biogenesis Group, Department of Chemistry, Indiana University, Bloomington, IN 47401

Following the method of Hinkle, Kim and Racker [J.B.C. 247, 1338 (1972)], a phospholipid vesicle preparation was obtained into which highly purified cytochrome *c* oxidase from yeast (seven subunits) could be incorporated. The properties of the preparation are similar to those of one using the beef heart enzyme. The enzyme incorporated in the vesicles seems to be generally less sensitive than its free counterpart to changes of the medium, such as salt concentration or pH; however, the activity is increased by sucrose to a greater extent when the enzyme is in the vesicles than when it is in the free state. Respiration coupling is higher when vesicles are reconstituted at room temperature (25°) than in the cold (4°), but coupling of vesicles prepared in the cold is increased by further standing at room temperature for a few hours, and this seems to be due to a reaccomodation of the enzyme within the vesicles. These properties will be compared with those exhibited by more highly resolved (five and four subunits) preparations.

**TH-PM-D10** EFFECT OF ENERGIZATION ON CYTOCHROME c OXIDASE OXYGEN INTERMEDIATES. H.J. Harmon, B. Chance and M.K.F. Wikström*. Johnson Research Foundation, School of Medicine, University of Pennsylvania, Philadelphia, PA. 19174 USA.

Using low temperature trapping procedures described previously (1), the effect of energization by ATP on cytochrome oxidase intermediates was studied. Addition of ATP to CO-inhibited pigeon heart mitochondria at room temperature induces energization as evidenced by reversed electron transfer. Trapping the energized state at -100° in the absence of $O_2$ followed by flash photolysis causes a 3-5 fold decrease in half-time of CO recombination with the reduced enzyme as compared to FCCP-treated membranes. Addition of $O_2$ to energized membranes at -30° does not cause replacement of CO. At -110° such energized membranes exhibit a 5 fold increase in rate of formation of Compound A ("oxy" compound) as compared to FCCP-treated membranes. Furthermore, the rate of conversion of Compound A to B ("peroxy" compound) is accelerated 5 fold. No differences in intermediate composition have been observed with ATP or FCCP but the rate of formation of Compound A and its conversion to Compound B are affected. At warmer temperatures, energized membranes exhibit 5 fold slower rates of cytochromes a, c and $c_1$ oxidation compared to FCCP-treated membranes. The following mechanism summarizes the effects of ATP on cytochrome oxidase:

$$O_2 \xrightarrow{\uparrow} A(a_3^{Cu^{1+}} \cdot O_2) \xrightarrow{\uparrow} B(a_3^{Cu^{2+}} \cdot O_2^{=}) \xrightarrow{\downarrow} \text{cyt } a \xrightarrow{\downarrow} \text{cyt } c{+}c_1$$

Here we find ATP effects upon the active site of oxygen reduction in cytochrome oxidase. (This research was supported by USPHS GM-01997, HL-17826 and GM-12202.)

1. B. Chance, C. Saronio, and J.S. Leigh, Jr. Proc. Natl. Acad. Sci. 22, 1635, 1975.

**TH-PM-D11** PROBES OF MEMBRANE ENERGIZATION AT SUBZERO TEMPERATURES IN APROTIC SOLVENTS. B. Chance, C.P. Lee, P.L. Dutton. Johnson Research Foundation, School of Medicine, University of Pennsylvania, Philadelphia, PA. 19174 USA.

Trapped states of energized membranes are observed in mitochondria (1-3), chloroplasts (4) and chromatophores (5). The kinetics of acquisition of the energized state at low temperatures may resolve localized and delocalized charge separations in and across the membrane (6). The oxonol dye, MC-V (7), is tightly bound to submitochondrial particles (SMP) (7:1 cyt. c:a ratio) and they are energized a) by NADH addition to the oxidized state or b) by flash photolysis of the reduced CO-inhibited state in the presence of oxygen, 25% ethylene glycol being present. In (a) electron transfer and energy coupling appear to be simultaneous down to -15° ($t_{1/2}$=25 s). In (b) at -18°, cyt. c oxidation is simultaneous with only the first phase of the biphasic response of the probe ($t_{1/2}$=2 and 10 s). The light-activated Rps. sph. chromatophores exhibit probe responses that are inhibited by antimycin A, activated by ethylene glycol (K≈0.8 M), increased alkalinity (pH≈8.2) and redox mediation (<0.5 mM ascorbate, pH 8.2). The temperature coefficient of the probe response in Rps. sph. is much greater than in SMP ($t_{1/2}$=34 s at -6°). The low temperature method affords the possibility of assigning localized and delocalized charge separation to specific segments of the electron transport chain. (Support from USPHS GM-12202, NINDS-10939, and HD-06274.)

1) B. Chance & B. Schoener, J. Biol. Chem. 241:4567, 1966. 2) B. Chance, M. Wikström & J. Harmon, in Electron Transport Chains & Oxidative Phosphorylation, Elsevier, Amsterdam, in press. 3) J. Harmon, B. Chance & M. Wikström, These Abstracts. 4) P. Mathis, Vth Internl. Biophys. Congr., Symp. 7, 1975. 5) P.L. Dutton, Biochim. Biophys. Acta 226:61, 1971. 6) B. Chance & M. Baltscheffsky, in Biomembranes, Vol. 7, Plenum Publ. Corp., New York, 1975, p. 33. 7) J. Smith and B. Chance, These Abstracts.

**TH-PM-E1** NANOSECOND TIME-DEPENDENT FLUORESCENCE ANISOTROPY OF PROBES ADSORBED TO BILAYER LECITHIN VESICLES. J.H. Easter*, R.E. Dale*, L. Chen*, and L. Brand, Biology Department, The Johns Hopkins University, Baltimore, Maryland 21218.

Nanosecond time-dependent emission anisotropy measurements of 2-p-toluidinonaphthalene-6-sulfonate (2,6 p-TNS) adsorbed to lecithin vesicles have been obtained at -1°C, 7°C, 20°C and 32°C. The apparent zero time anisotropy ($A_0$) decreases with increasing temperature, suggesting a small temperature-dependent angular motion of the probe on the sub-nanosecond time scale. At -1°C, 7°C and 20°C the limiting anisotropy at long times is not zero. The limiting anisotropy decreases as the temperature is increased and is zero at 32°C. Thus the rotational freedom of the dye at the bilayer binding-site appears to be restricted at the lower temperatures. The decay of the emission anisotropy cannot be described by a first order rate law suggesting that the freedom of rotation within the binding site may be anisotropic. However the possibility of more than one type of binding site has not been excluded. The time-dependent emission anisotropy of 2,6 p-TNS adsorbed to human erythrocyte ghosts at 7°C is similar to that with the vesicles in that the limiting anisotropy is not zero and the decay of the anisotropy cannot be described by a single exponential. In contrast to the difficulties associated with the interpretation of steady-state polarization experiments, nanosecond time-resolved measurements are capable of resolving the contributions of viscous opposition to rotational motion of probes in membranes and providing information regarding restrictions to their range of rotational freedom. (Supported by NIH grants No. GM11632, GM10245, GM-5T01-G57 and NSF grant No. GB-37555).

**TH-PM-E2** THE USE OF SURFACE SPIN LABELS IN THE STUDY OF MEMBRANES. J.R. Lepock*, A.M. Mastro, and A.D. Keith, Department of Biochemistry and Biophysics, The Pennsylvania State University, University Park, PA 16802

Several amphipathic esr spin labels have been synthesized. They are long molecules of the form - hydrocarbon chain:charged group:nitroxide ring. The charge can be positive or negative. In the charged form the spin labels are impermeable to cells (1). Therefore they probe only the plasma membrane and should be useful when only this membrane is of interest. The hyperfine coupling constant for these spin labels when in membranes is between that found when the labels are in oil and in water, indicating that they are in a region of intermediate polarity. The nitroxide moiety must reside somewhere between the hydrocarbon zone of the lipid bilayer and the water surrounding the membrane. This is the polar surface region of the membrane and we therefore call these surface spin labels to distinguish them from the commonly used hydrocarbon spin labels.

The addition of $Ca^{++}$ to phosphatidyl choline multi-bilayers has very little or no effect upon the spectrum of hydrocarbon spin labels when the bilayer is in the fluid state. The spectrum of the surface labels indicates an increase in the rigidity of the surface polar regions after the addition of $Ca^{++}$. Thus $Ca^{++}$ can bind to and influence the properties of neutral phospholipids. Studies are now being conducted to determine whether differences can be detected by use of the surface labels between the surfaces of virus infected, transformed and normal mammalian cells.

(1) Lepock, J. R., Morse, P.D., Mehlhorn, R.J., Hammerstedt, R.H., Snipes, W. and Keith, A.D. FEBS Letters (in press).

**TH-PM-E3** MEMBRANE MOTIONS OBSERVED DIRECTLY BY ELECTRON MICROSCOPY AND ELECTRON DIFFRACTION. S. W. Hui, Electron Optics Laboratory, Roswell Park Memorial Institute, Buffalo, N.Y. 14263.

The motions of electron-opaque marker particles on membranes have been recorded and measured. Corresponding changes in the electron diffraction patterns are also observed. The membrane specimens are kept in a fully hydrated condition at controllable temperatures by the use of an environmental stage in an electron microscope[1]. The sub-micrometer size gold particles and latex spheres are attached to single lipid bilayers and plasma membrane ghost vesicles. The fast, Brownian-like, random motion is recorded by prolonged exposures of 5 seconds, while the coordinated drift of groups of particles is recorded by exposures at 15 seconds intervals. The mean square displacements are measured and the apparent diffusion coefficients are deduced. These quantities are measured as functions of temperature, and also functions of the known compositions in the case of synthetic bilayers. Abrupt changes in the motion of the marker are observed at the transition temperatures. The diffusion coefficients of an equimolar mixture of cholesterol and dipalmitoyl lecithin bilayer are circa $10^{-9}$ $cm^2/sec$ and $10^{-11}$ $cm^2/sec$ respectively at 20°C and 4°C. The data are comparable to those from NMR and spin lable ESR experiments[2]. The coordinated drift of micrometer-size patches below the transition temperature agrees with the domain model observed by electron diffraction[3] and diffraction contrast electron microscopy[4]. ref: (1) Hui, Hausner and Parsons, J. Phys. E. in press. (2) Edidin, Ann. Rev. Biophys. Bioeng. 3, 179, 1974. (3) Hui, Parsons & Cowden, Proc. Natl. Acad. Sci. 71, 5968, 1974. (4) Hui and Parsons, Science 190, 383, 1975.

**TH-PM-E4** THE STRUCTURE OF ORIENTED SPHINGOMYELIN BILAYERS. R.S. Khare and C.R. Worthington
Departments of Biological Sciences and Physics, Carnegie-Mellon University, Pittsburgh, Pa. 15213

A brief review of the previous x-ray diffraction studies on sphingomyelin (SM) and related derivatives will be presented. Using Silane surfactant N,N-dimethyl-N-octadecyl-3-aminopropyltrimethoxysilyl chloride (kindly provided by Dr. E.P. Plueddman of Dow Corning Corp.), oriented samples of SM were prepared by slow evaporation from organic phase in glass capillaries. X-ray diffraction from these samples gave up to 14 orders of lamellar reflections, of the basic repeat of 68.5 Å and up to 8 reflections, including an intense one at 4.2 Å, at right angles to the lamellar reflections. The lamellar reflections derive from SM bilayers. The diffraction spacings did not change when these SM bilayers in capillaries were exposed to atmosphere of high or low relative humidities even for an extended periods of time. X-ray analysis using various electron density strip models for SM bilayers have been tested with the lamellar diffraction data. We find that the Patterson function of SM bilayers can be directly interpreted. The molecular structure of SM in oriented bilayers resembles the structure of 1,2 dilauroyl-dl-phosphatidylethanolamine in crystal form (Hitchcock et al 1974, PNAS 71,3036). Our studies indicate: (1) the hydrocarbon chains in SM bilayers are straight and nearly parallel to each other, (2) polar head group is curled up and (3) there is only a limited interdigitation of hydrocarbon chains of the adjacent SM molecules in the bilayer. Fourier synthesis of the SM bilayers at a resolution of about 2.5 Å will be presented.

**TH-PM-E5** X-RAY DIFFRACTION ANALYSIS OF ORIENTED LIPID BILAYERS. T.J. McIntosh, R.C. Waldbillig*, and J.D. Robertson, Department of Anatomy, Duke University School of Medicine, Durham, North Carolina, 27706.

Well oriented fatty acid bilayers formed by the dipping procedure of Langmuir and Blodgett have been analyzed by wide-angle and low-angle x-ray diffraction techniques. The wide-angle diffraction spots have given direct information on hydrocarbon chain packing and chain tilt. It has been determined that the chain packing is orthorhombic and the tilt for several different fatty acids is 27° relative to the normal to the plane of the bilayer. Associating an alkali earth cation to the carboxyl headgroup significantly reduces the chain tilt, with each cation producing a different arrangement of hydrocarbon chains. The lamellar low-angle diffraction patterns, which for particularly well ordered specimens contain as many as 25 reflections, have been interpreted by use of an isomorphous replacement technique. Electron density profiles have been computed at 6Å resolution on an absolute electron density scale for several fatty acids and their salts. These profiles have been correlated with electron micrographs of the same unfixed, unstained samples. In addition, the hydrocarbon chain region of the bilayer has been modified in various ways. Hydroxyl groups have been situated at selected locations along the chains to produce local increases in electron density. Diffraction data have been collected and analyzed for bilayers composed of unsaturated fatty acids--both before and after exposure to bromine vapor, for bilayers composed of a mixture of different fatty acids, and for bilayers of well defined chemical asymmetry. Electron density profiles will be presented for bilayers asymmetric with respect to both head group and chain length.

**TH-PM-E6** ALKANE SOLUBILITY IN PHOSPHOLIPID BILAYERS. S.A. Simon*, W.L. Stone,* and P. Busto-Latorre*, Departments of Physiology and Biochemistry, Duke University, Durham, North Carolina 27710. (Intr. by George Padilla).

The partition coefficients of n-hexane between water and unsonicated dispersions of DPL, DML, and DOL were measured as a function of temperature. For the saturated lipids alkane partition was found to be maximum near the phase transition temperature with unitary free energies of n-hexane transfer of -7.07 and -6.30 kcal/mole for DPL and DML, respectively. Although a pretransition peak was observed for DPL and DML the solubility of n-hexane drops precipitously at temperatures below $T_m$. Above 27°C the free energy of transfer was similar for DOL and DML.

The Van't Hoff plot for DOL differs significantly from that observed for the saturated lecithins above $T_m$. For DOL the enthalpy of transfer decreases with increasing temperature whereas for DPL and DML the enthalpy was found to increase with increasing temperature. The results for DOL are characteristic of hydrophobic interactions found in other systems, e.g., liquid hydrocarbon and detergent micelles. The anomalous results for the saturated lipids probably reflect an ordering of the hydrocarbon tails occuring before the phase transition.

The addition of cholesterol to DPL at a 2:1 DPL: cholesterol mole ratio resulted in an increase in the partition coefficient of hexane below $T_m$ and a decrease above $T_m$ relative to a pure DPL bilayer. With this mixture the partition coefficient was independent of temperature. This work was funded by grants HL-12157 and ONR Contract No. N0014-67-A-021.

**TH-PM-E7** LIPID PHASE EQUILIBRIA AT HIGH PRESSURE. William Z. Plachy, Chemistry Department, San Francisco State University, San Francisco, California 94132

The crystalline - liquid crystalline phase transition temperature for aqueous dispersions of three synthetic lipids (dimyristoyl, dipalmitoyl and distearoyl phosphatidylcholine) has been determined to 70°C at pressures up to 2500 atm. The transition is observed at constant temperature with increasing pressure in a high pressure ESR cell by monitoring the partitioning of the di-tert-butyl nitroxide free radical between lipid bilayers and the aqueous medium. The transition is reversible within experimental error and has a width of about 40 atm at all pressures.

At moderate pressure ($P \leq 800$ atm) the slope, dP/dT, is pressure independent and in the range 42±4 atm/deg for all three lipids. The slope appears to decrease with increasing chain length. This slope is consistent with that predicted by the Clapeyron equation using known 1 atm $\Delta V$ and $\Delta H$ values for the dipalmitoyl lipid. At higher pressures dP/dT increases by as much as 40% for the dimyristoyl lipid at 2500 atm.

The slope, dP/dT, for the pre-transition of dipalmitoyl phosphatidylcholine is 100±15 atm/deg. This value is also consistent with the Clapeyron equation. The pre-transition event becomes undetectable with our technique above 1000 atmospheres.

**TH-PM-E8** OPTICAL STUDIES OF MONODOMAIN PHOSPHOLIPID BILAYERS CONTAINING VARIOUS BIOLOGICAL MEMBRANE COMPONENTS.† L. Powers†† and P.S. Pershan*, Gordon McKay Laboratory, Harvard University, Cambridge, Cambridge, Mass. 02138

Using methods similar to those described in previous papers for the orientation of phospholipid bilayers,[1] other biological membrane components such as cholesterol, chlorophyll, and antibiotics may be incorporated and macroscopic monodomain samples produced. Likewise, additional water may be added (up to the one phase limit) in the Lα (smectic A) phase. Refractive indices of these systems have been studied in the temperature range ($80°C \leq T \leq 20°C$) for various hydrations (2-30% wt). This data has been used to construct a phase diagram for cholesterol + dipalmitoyl phophatidylcholine (DPPC) + water system as a function of temperature. Samples containing chlorophyll a (.001 - .05 chlorophyll/lipid molar ratio) incorporated in DPPC bilayers show no biaxial birefringence while linear dichroism shows that the chlorophyll molecules (.01 molar ratio) are oriented in the bilayer plane for water concentrations less than ~ 10% wt. The antibiotics valinomycin, nonactin and gramicidin A have been incorporated in monodomain phospholipid bilayers (max ~ 1/50 molar ratio). Only samples containing gramicidin A showed biaxiality at low (~ 5% wt) water. At high water content the uniaxial birefringence of these antibiotic containing samples is very low (< .015).

[1]L. Powers and N. A. Clark, PNAS 72 (1975), 840.

†This work was supported by NSF Grant No. DMR72-03020-A05 and DMR72-02088.
††Supported by NIH Training Grant No. 5-T01 GM00782-15.

**TH-PM-E9** OPTICAL STUDIES OF MONODOMAIN PHOSPHOLIPID BILAYERS.† L. Powers,†† J.P. LePesant,* and P.S. Pershan,* (Intr. by James L. Ellenson) Gordon McKay Laboratory, Harvard University, Cambridge, Mass. 02138

In recent papers,[1] methods were discussed for the macroscopic orientation of phospholipid bilayers containing small (2-8% weight) water concentrations. These preparations are single domain smectic liquid crystals typically 1 $cm^2$ in area and up to 500 μ thick. Additional water (up to the one phase limit) may be incorporated after the bilayers are aligned and in the Lα (smectic A) phase. The refractive indices of these samples have been studied as a function of temperature ($90°C \leq T \leq 20°C$) and degree of hydration (2-30% wt) at wavelength $\lambda = 632.8$ nm and this data was used to construct a phase diagram for dipalmitoyl phophatidylcholine. A striking feature of this phase diagram is the transition that appears at ~ 20% wt water for $T > 43°C$ and was first reported by Gary-Bobo.[2] The changes in refractive indices are indicative of changes in the hydrocarbon chains except for a biaxial region (2-13% wt water). Monovalent and divalent cations have also been added to the monodomain samples and their effect investigated with birefringence. Brillouin scattering has been used to measure the elastic constants associated with compression of the bilayers as a function of direction, temperature, and water content.

[1]L. Powers and N. A. Clark, PNAS (USA) 72 (1975), 840.
[2]C. M. Gary-Bobo, Y. Lange, and J. L. Rigaud, BBA 233 (1971), 243.

†This work was supported by NSF Grant No. DMR72-03020-A05 and DMR72-02088.
††Supported by NIH Training Grant No. 5-T01 GM00782-15.

**TH-PM-E10** CHARACTERISTICS OF PHOSPHATIDYLETHANOLAMINE IN AQUEOUS DISPERSIONS. M. Waite, A.D. Bangham*, and N. Miller*, Dept. of Biochemistry, The Bowman Gray School of Medicine, Winston-Salem, N. C. 27103 and The Institute of Animal Physiology, Babraham, Great Britain

Smectic mesophases (multishell liposomes) of pig liver phosphatidylethanolamine (PE) were prepared in aqueous media by sonication. When titrated with HCl, the amine had a $pK_{obs}$ of 10.0 and was titrated over a wider range of pH values than expected. The unusual titration curve we ascribe to the close proximity of the amines in the liposomes plus the effect of the electronegative phosphate on the PE molecule. When mixed in liposomes with phosphatidylcholine (PC) no titratable groups were found. However, the addition of a proton carrier (FCCP) or Triton allowed titration of the PE amine. Likewise, mixed liposomes of PE and PC did not migrate in an electrical field whereas liposomes of pure PE had a negative charge at neutral pH. We believe that the negative charge on PE liposomes is in part the strong interaction of the amine with anions, relative to PC (Zull, J.E., and Hopfinger, A.J., 1969, Science 165, 512). Our data indicate PE is buried within the liposome whereas PC forms the outer layer of the liposome. The outer layer of PC in the liposome could be either an entire bilayer or simply the outer monolayer of the bilayer. Above 1 mM concentrations, KCl decreased the mobility of PE liposomes as predicted by the Gouy-Chapman equation. $CaCl_2$, on the other hand, caused the liposome to have a positive charge, though this was reduced by the addition of KCl. The effect of $CaCl_2$ on the mobility of PE liposomes was pH dependent; $CaCl_2$ had no influence at pH values where the liposomes were not negatively charged, and had maximal effect when the amine was not protonated (i.e., at or above the pK). Supported by NIH grants AM11799 and CA14318.

**TH-PM-E11** POSSIBLE FALLACY IN THE USE OF THE ELECTRONEUTRALITY PRINCIPLE IN STUDIES ON VESICLES. W. S. Rehm, S. G. Spangler, G. M. Schoepfle, and G. Sachs, Department of Physiology and Biophysics, University of Alabama in Birmingham, Birmingham, Alabama 35294

Although there is a violation of electroneutrality in the presence of a transmembrane potential difference (PD), it is usually assumed that the quantity of ions involved in the violation is too small to be detected chemically. We present a hypothetical experiment indicating this assumption may not always be true in the case of reconstituted membrane vesicles, the reason being that small vesicles provide a large surface to internal volume ratio. Consider a vesicle (spherical, with external radius r and internal radius b) which has conductive pathways for only one species of ion (a monovalent cation $B^+$). Initially $[B^+]$ = 1 mEq/l both inside and out (larger quantities of other electrolytes are also present), and the transmembrane PD = 0. Now let a PD be established (e.g., by a step increase in outside $[B^+]$ or by activation of an electrogenic pump) such that the inside of the membrane is made positive. $B^+$ will move inward until the vesicle, viewed as a spherical capacitor, is charged. The net charge moving into the vesicle = CV where C is the capacitance of the membrane and V is the PD; hence $\Delta[B^+]$ = CV/vF where v is the internal volume ($4\pi b^3/3$) and F is the Faraday. C(mks system) for a spherical capacitor = $4\pi\varepsilon rb/(r-b)$ where $\varepsilon$ is the dielectric constant of the material comprising the membrane. If $\varepsilon$ = $50 \times 10^{-14}$ f $cm^{-1}$ (so that $C_f$ for a flat membrane $50 \times 10^{-8}$ cm thick is $10^{-6}$ f $cm^{-2}$), then $\Delta[B^+]$ in Eq/l = $155.4 \times 10^{-16}$ $rV/b^2(r-b)$ where r and b are in cm and V is in volts. For V = 0.1 and (r-b) = $50 \times 10^{-8}$, the $\Delta[B^+]$ for vesicles 0.1; 0.05 and 0.02 μm in diameter is 0.77; 1.9 and 12.4 mEq/l respectively, values which should be chemically detectable. Other situations involving conductive pathways for both $B^+$ and $H^+$ will be discussed. (NIH and NSF support.)

**TH-PM-E12** POTENTIAL DEPENDENT ABSORPTION CHANGES OF CYANINE AND OXONOL DYES ON BLACK LIPID MEMBRANES. A. Waggoner, C.-H. Wang and R. L. Tolles, Department of Chemistry, Amherst College, Amherst, Massachusetts 01002.

Glycerol monoolein bilayer membranes were used to study the dependence of cyanine and oxonol dye light absorption on transmembrane potential. For the cyanine dye diS-$C_2$-(5) a change in absorption of 5 parts in $10^{-5}$ was observed at 670 nm. Potential steps of up to ±100 mV centered about 0 mV (ground) produced no response but steps from 0 mV to either +100 mV or to -100 mV produced an absorption decrease at 670 nm, which had a fast rise time of $\tau_f \lesssim 25$ μsec. However, the signal did not appear immediately after the 1 msec potential steps were applied to the membrane. Instead the optical signal appeared with a slower time course varying from $\tau_s$ < 1 sec to $\tau_s \approx 40$ seconds, depending on the dye used. For the N-ethyl substituted cyanine dye, diS-$C_2$-(5), $\tau_s \approx 40$ sec, and for the N-pentyl derivative diS-$C_5$-(5) $\tau_s$ < 1 sec. When $\tau_s$ was large, the membrane current carried by the charged dye was found to be low. We propose that dye initially added to both sides of the membrane is locally depleted on one side of the membrane and locally concentrated on the other side with a time constant to $\tau_s$ after the potential steps are initiated. The rapid ($\tau_f$) response is due to the potential dependent movement of dye between the membrane and the aqueous phase on the high concentration side of the membrane. Absorption experiments with the dyes in model solvents and phospholipid vesicles indicate that when low concentrations ($10^{-6}$ M) of dye are used, monomer dye in the membrane moves to form dimers in the aqueous phase as the potential steps go positive or negative from ground. The mechanism of the change of oxonol dye absorption with membrane potential appears to be similar.

TH-PM-E13 AC STUDIES OF PESTICIDE INDUCED CHARGE TRANSPORT IN LIPID BILAYERS. A.D. Pickar,* Intr. by K. Hsu, Department of Physics, Portland State University, Portland, Ore. 97207.

The ac conductances and capacitances of lipid-cholesterol membranes treated with pentachlorophenol (PCP) have been measured in the range 0.1 to 100 kHz. In making these measurements it is necessary that the resistance of the aqueous environment, which is a buffered KCl solution, be evaluated for individual membranes by an extrapolation procedure at high frequencies. The results, given in terms of loss tangent vs. frequency curves, are corrected for high frequency dielectric loss, the presence of which is incidental to the charge transport mechanism under study. The loss tangent curves show that the membrane can be represented by a three element equivalent circuit in which the properties of the two surfaces and of the interior are given in terms of frequency independent resistors and capacitors. Values of interior conductivity which are thus obtained agree with net conductivity measurements made by dc methods. The dependence of surface conductivity on pH and PCP concentration is consistent with the dimer scheme of charge transport derived from dc measurements, and also sheds further light on details of the mechanism such as binding site saturation. Surface capacitances vary linearly with PCP concentration and are also dependent upon pH; values range between 15 and 90 times that of the interior capacitance. Supported by NIH Grant ES 937.

TH-PM-E14 MEMBRANE FUSION IN PHOSPHOLIPID SPHERICAL MEMBRANES. W. Breisblatt, and S. Ohki, Mt. Sinai Medical School, New York, NY and Dept. of Biophysical Sciences, State University of New York at Buffalo, Amherst, NY 14226.

Effect of cholesterol, divalent ions and pH on spherical bilayer membrane fusion was studied as a function of increasing temperature. Spherical bilayer membranes were composed of natural (phosphatidyl choline-PC, and phosphatidyl serine-PS) as well as synthetic (dipalmitoyl-PC, dimyristoyl-PC and dioleoyl-PC) phospholipids. Incorporation of cholesterol into the membrane (33% by weight) abolished the fusion temperature and also greatly reduced the percentage of membrane fusion. The presence of 1 mM divalent ions ($Ca^{++}$, $Mg^{++}$ or $Mn^{++}$) on both sides or one side of the PC membrane did not affect appreciably its fusion characteristic with temperature, but the PC membrane fusion with temperature was greatly enhanced by the presence of divalent ions. The variation of pH of the environmental solution in the range of 5.5 $\sim$ 7.0 did not affect the membrane fusion characteristic. However, at pH 8.5, the fusion with respect to temperature was shifted toward the lower tempera ture by approximately 3°C for PC and PS membranes, and at pH 3.0 the opposite situation was observed as the fusion temperature was increased by 6°C for PS membrane and by 4°C for PC membrane. Also, the degree of the above fusion was compared with the expansion of monolayer with increasing temperature. It is concluded that membrane fluidity, structural instability and hydrophobic interaction between the membranes are important for membrane fusion to occur.

TH-PM-E15 THE INTERACTION OF PHOSPHOLIPID VESICLES WITH BLACK LIPID MEMBRANES. N. Düzgüneş and S. Ohki, Department of Biophysical Sciences, State University of New York at Buffalo, Amherst, N.Y. 14226

The electrical properties of black lipid membranes made of phosphatidylserine-decane, incubated in the presence of a suspension of unilamellar phospholipid vesicles in the aqueous compartment bathing one side of the membrane, are investigated. When $Ca^{2+}$ is introduced to a phosphatidylcholine vesicle suspension, a simultaneous increase in and fluctuations of the planar membrane are observed. The fluctuations are in steps or spikes over an average base level conductance, which is at least an order of magnitude higher than the initial level. Phosphatidylserine vesicles do not cause such fluctuations, whereas vesicles made of a 1:1 mixture of phosphatidylcholine and phosphatidylserine have an effect similar to phosphatidylcholine vesicles. The effects of incubation time before the introduction of $Ca^{2+}$ and the concentration of $Ca^{2+}$ on the conductance will be reported. The results are discussed in terms of membrane adhesion and fusion, with respect to studies on fusion between spherical bilayers (Breisblatt & Ohki, J. Membrane Biol. 23:385,1975; J. Colloid Interface Sci., submitted), vesicles (Papahadjopoulos et al., BBA 352:10,1974; BBA 394:483,1975) and between liposomes and planar membranes (Pohl et al., BBA 318:478, 1973).

**TH-PM-E16** PLANAR LIPID BILAYERS AS MODEL TARGETS FOR THE C5b-9 COMPLEMENT ATTACK MECHANISM. D.W. Michaels, A.S. Abramovitz*, and M.M. Mayer*; Departments of Physiological Chemistry and Microbiology, Johns Hopkins Univ. School of Medicine, Baltimore, Md. 21205.

We have found that the electrical conductance of planar lipid bilayers increased (ca. 5-10x) upon treatment with nanogram quantities of purified C5b,6 complex and complement components C7 and C8. Addition of C9 greatly amplifies this conductance change (ca. 100-1000x). No increase in baseline conductance was observed when components were added solo to the membrane, or when used in paired combinations, or when C5b,6, C7, C8, and C9 were admixed prior to addition. Thus, there is a significant parallel between the conductance changes induced in the model membrane by the C5b-9 complement attack mechanism and damage produced by these factors in biological membranes and liposomes. The electrical properties of C5b-9 treated membranes displayed several features characteristic of putative channel-formers (e.g., alamethicin and gramicidin). First, membrane conductance increased with time in a disjunct manner. Second, the steady-state conductance increased exponentially with voltage. Finally, no conductance changes were observed in thick films. We conclude that planar lipid membranes constitute an excellent model system for studies on the mechanism of the cytolytic action of complement. (Supported in part by U.S.P.H.S. Grant #5 ROI AI-02566-17, NSF Grant GB38628 awarded to M. M. Mayer and U.S.P.H.S. Grant GM05919 awarded to Albert L. Lehninger.)

**TH-PM-F1** PROTON MAGNETIC RESONANCE STUDIES OF DINUCLEOSIDE MONOPHOSPHATES. SIGNAL ASSIGNMENTS AND CONFORMATIONAL ANALYSIS. F. S. Ezra and S. S. Danyluk, Division of Biological and Medical Research, Argonne National Laboratory, Argonne, Illinois 60439, C. H. Lee* and R. H. Sarma*, Department of Chemistry, State University of New York at Albany, Albany, N.Y. 12222, N. S. Kondo, Department of Chemistry, Federal City College, Washington, D.C. 20005.

A detailed proton magnetic resonance study of the conformations of fifteen dinucleoside monophosphates in solution has been completed. Selectively deuterated dimers were synthesized and used in a direct assignment of the pmr signals. Chemical shifts and spin-spin coupling constants were then measured from the spectra of the fully protonated dimers and refined by computer simulation. The C3'-endo ribose ring, g-g, g'-g' conformations about the C4'-C5', C5'-O5' bonds and g⁻ about the C3'-O3' bond are prevalent in all the dimers. Significant changes occur in the ribose ring structures and in the flexibility about the C4'-C5' and C5'-O5' bonds of the nucleotidyl residues upon dimerization. Estimates of the degree of intramolecular stacking are made from the ribose ring coupling constants and are found to vary from 10% in UpG to 50% in GpC at 18°C. Other structural features such as base-ribose ring orientation and conformations about the phosphorus-ester oxygen bonds have been qualitatively deduced from the chemical shifts. Base sequence is observed to have a profound effect on the overall conformation.

Acknowledgment: This research was supported by the U.S. Energy Research and Development Administration, National Cancer Institute and MBS program of NIH and the National Science Foundation.

**TH-PM-F2** CONFORMATIONAL DYNAMICS OF URIDYLYL-(3'-5')-ADENOSINE IN SOLUTION:PROTON $T_1$ MEASUREMENTS. A. M. Wyrwicz* and S. S. Danyluk, Division of Biological and Medical Research, Argonne National Laboratory, Argonne, Ill. 60439.

An extensive study has been made of proton spin-lattice relaxation times ($T_1$) for uridylyl-(3'-5')-adenosine, UpA, in $D_2O$ over a range of temperature and pD. The measurements show that $T_1$ values of UpA are dominated by a dipole-dipole relaxation mechanism. Utilization of two selectively deuterated analogues, 5,6,1',2',3',4',5',5"-octadeuteriouridylyl-(3'-5')-adenosine and uridylyl-(3'-5')-2,1',2',3',4',5',5"-heptadeuterioadenosine has made it possible to sort out intra-base contributions to intramolecular dipole-dipole interaction. For base and anomeric H1', the $T_1$ ratio H8:H1' and H6:H1' is given to a reasonable approximation by

$$(T_1)_{8(6)}/(T_1)_{1'} \simeq \sum_{i \neq 8(6)} r\ (8(6), i)^{-6} / \sum_{i \neq 1'} r(1', i)^{-6}$$

where r (8(6),i) and r (1',i) represent distances from H-i to H-8(6) and H-1', respectively, assuming identical correlation times. Analysis of these ratios confirms an *anti* glycosidic bond orientation for both nucleotidyl moieties over the temperature and pD range covered in this study. Finally, using the $T_1$ data in combination with X-ray structure results specific microdynamic models are proposed for the motion of UpA in solution.

Acknowledgment: This research was supported by U.S. Energy Research and Development Administration.

**TH-PM-F3** OPTICAL ACTIVITY OF URIDYLYL-(3'-5')-ADENOSINE. CRYSTAL STRUCTURE AND SOLUTION CONFORMATION. N.P. Johnson, E. Switkes*, and T. Schleich, Division of Natural Sciences, University of California, Santa Cruz, California 95064.

Circular dichroism and absorption spectra have been calculated for protonated and unprotonated UpA in each of the two observed crystal structures and two model polynucleotide conformations. Both the Tinoco coupled oscillator and generalized susceptibility formalisms were used. The coupled oscillator calculation was performed with two differently parameterized PPP wavefunctions and also experimental transition properties. The methods give very similar results for consistent values of transition energies, polarizations, and oscillator strengths. Spectra calculated with experimental data for both protonated and unprotonated UpA in the polynucleotide conformations are consistent with observed results. Calculated spectra for protonated UpA in one of the crystal structures also matches experiment. For unprotonated UpA, however, calculated spectra for both crystal geometries disagree with experiment and consequently these structures are probably minor contributors to the distribution of conformations this molecule assumes in neutral aqueous solution. PPP calculations for both parameterizations predict that the red shift in the absorption spectrum of adenine observed at low pH arises from the enhancement of a previously weak low energy transition. (Supported by National Science Foundation grant BMS75-17114 to T.S. and a grant from Petroleum Research Fund to E.S.)

**TH-PM-F4** CONFORMATIONS OF DIDEOXYRIBONUCLEOSIDE PHOSPHATES BY CLASSICAL POTENTIAL ENERGY CALCULATIONS. S. Broyde and R. M. Wartell, School of Physics, Georgia Institute of Technology, Atlanta, Ga. 30332, and S. D. Stellman,* American Health Foundation, N.Y., N.Y.10019. Classical potential energy calculations have been made for dGpdC, as well as for a number of other dideoxyribonucleoside phosphates. In these calculations the energy was minimized with the eight dihedral angles and the sugar pucker as variable parameters. Van der Waals, electrostatic, torsional and deoxyribose ring strain contributions to the energy were included. The three staggered conformations of $\psi$ were examined, together with all combinations of the staggered regions of $\omega'$ and $\omega$. Low energy conformations like helical DNA were found, as well as low energy conformations that introduce a turn when incorporated in the helical polymer. For dGpdC the A form is the global minimum. It has dihedral angles like GpC, and like A-DNA and A-RNA fibers; the sugar pucker is C-(3') endo envelope. The C-(2') endo - C-(3') exo B-like conformation is at 0.2 kcal/mole. This calculated dGpdC conformation has a rotation per residue of 41°, which is comparable to the value of 45° evaluated from fiber data of the D form of $(dG\text{-}dC)_n\cdot(dG\text{-}dC)_n$.[1] Another low energy conformation in the C-(2')-endo region at 0.6 kcal/mole, has $\omega', \omega$ $g^-t$ and $\psi$ near 180°. Conformational features of other sequences will also be discussed.

1. S. Arnott, R. Chandrasekaran, D. Hukins, P. Smith and L. Watts, J. Mol. Biol. 88, 523 (1974).

**TH-PM-F5** POSSIBLE HELICAL STRUCTURES FOR NUCLEIC ACIDS AND POLYNUCLEOTIDES. N. Yathindra* and M. Sundaralingam, Department of Biochemistry, University of Wisconsin, Madison, Wisconsin 53706.

To analyze the possible helical structures for nucleic acids and polynucleotides, the helical parameters-n, number of nucleotide residues per turn and h, the height per residue-are evaluated for C(3') endo and C(2') endo class of sugars based on the rigid nucleotide concept. These (n-h) plots obtained as a function of internucleotide P-O(3') ($\omega'$) and P-O(5') ($\omega$) torsions exhibit similar shapes but with a shift along $\omega'$ and $\omega$ directions depending upon the nature of the sugar pucker and C(4')-C(5') torsion. The helix forming domains correspond to low energy regions of the $(\omega',\omega)$ energy surface and interestingly they all lead to stacking for the anti base. The striking observation is that the (n-h) plots predict the stereochemical possibility of left-handed helices characterized by helical parameters similar to the observed right-handed helices. Both occur in the broad $g^-g^-$ domain indicating that relatively small torsion changes can lead to a variety of helical conformations. The observed polynucleotide helices (8-12 fold) also occur in the narrow $g^-g^-$ domain indicating the possibility of smooth interconversion. Model building studies suggest that the orientation of the base may have an important influence in discerning the helical sense and the stability of polynucleotide helices. These observations serve as a basis for the analysis of double helical and multistranded nucleic acid structures.

Supported by NIH Grant GM-17378.

**TH-PM-F6** THE ORDERED POLYNUCLEOTIDE CHAIN. HELIX FORMATION AND BASE STACKING. W.K. Olson, Department of Chemistry, Douglass College, Rutgers, the State University, New Brunswick, New Jersey 08903.

The helical parameters (z - the vertical displacement of adjacent residues along a rectilinear or helix axis, r - the radial distance of equivalent atoms from the helix axis, and $\theta$ - the cylindrical rotation angle about the helix axis between corresponding atoms of neighboring units) are well known to be functions of the spatial configuration of the six chemical bonds comprising a single repeating unit of the chain backbone. These parameters and hence the handedness of the helix depend in no way upon the glycosyl rotation connecting the base to the sugar-phosphate backbone. The stacking of bases in the ordered polynucleotide, however, is a function of the spatial orientation of both the chain backbone and the base atoms. A variety of stacked and unstacked structures can thus be associated with a single helical backbone. The familiar RNA-B helical backbone, for example, can accommodate either right-handed or left-handed base stacks as the glycosyl rotation assumes different orientations. Certain polynucleotide chains which exhibit left-handed base stacking patterns in nmr and CD studies may, in fact, describe right-handed helices.

**TH-PM-F7** SPIN LABELED RNAs ($RNA^{SL}$) AS PROBES OF VIRAL RNA STRUCTURE. A. Thomas Powell*, M. Gordon, L. Goetsch*, B. Byers*, Biochem. & Genetics, U. of Wash., Seattle, WA, J. Greene*, W. Caspary*, P. Ts'o, Div. of Biophys., Johns Hopkins U., Balt., MD. Intr. by B. Hall.

Homopolyribonucleotides were spin labeled using iodoacetamide nitroxide compound. The extent of labeling depends on the base and secondary structure, poly A and poly C being the most reactive. The spin label-polymer linkage was unstable in phosphate buffer and at high temp. The conformations of these $RNAs^{SL}$ were characterized by changes in the correlation times ($\tau$) of their attached spin labels under differing conditions of solvent, temp., viscosity, pH and salt. These studies indicated that $\tau$ and anisotropy factor of the esr signal reflects certain conformational states of the $RNA^{SL}$. In an extension of these basic studies, poly $A^{SL}$ was encapsulated by coat proteins of two plant viruses, tobacco mosaic virus (TMV), a rigid rod, and cowpea chlorotic mottle virus (CCMV), an icosohedron. The kinetics of encapsulation was followed by esr and uv. The fidelity of the final products was examined by isopycnic centrifugation in CsCl, electron microscopy (EM) and resistance to nuclease. The particles resembled their native viruses in the EM. The esr of TMV-poly $A^{SL}$ particle is largely isotropic, strongly immobilized, and showed a hyperchromic effect at 260 nm during encapsulation. These particles are insensitive to micrococcal nuclease as monitored by esr. In contrast, the esr spectrum of CCMV-poly $A^{SL}$ was not as strongly immobilized as TMV-poly $A^{SL}$ and a hypochromic effect was observed upon encapsulation. The particle is slightly sensitive to $T_2$ RNase suggesting that the RNA packaged within CCMV is more accessible to the external environment than within TMV. This use of spin labels as direct probes of the internal conformation and as indirect probes in conjunction with external agents provides new insight into the self assembly and RNA packaging of plant viruses. Supported by grants from NSF, ERDA, and AEC.

**TH-PM-F8** DYNAMIC MODEL OF tRNA AND ITS CORRELATION TO GENETIC TABLEAU, Okan Gurel, IBM Corporation, 1133 Westchester Avenue, White Plains, New York 10604.

Genetic tableau as announced in [O. Gurel, Biophys. J. Society Abstracts 9(1969) p.A254] refers to a rearrangement of the genetic code revealing certain structural groupings of the codons, thus the amino acids. The tRNA molecules play an important role in transferring the information from DNA to ribosomes. During the protein synthesis, anticodon portion (loop III of tRNA is suggested to interact with mRNA. A dynamic tertiary structure of this molecule has been proposed as interacting with ribosomal subunits and mRNA [O. Gurel, In: Proteins, Nucleotides, vol.I, 1st European Biophysical Congress (1971) 421-425]. In this functional model, four nucleotides located at specific portions of the tRNA (two in loop I and two in loop IV) are observed as playing a key role [O. Gurel, Physiol. Chem. Physics 5(1973)177-182] The 3' end of tRNA is suggested to interact with the amino acid residues. To date, however, there has been no role attached to the 5' end and the loop II (extra loop!) of tRNA in connection with protein synthesis. Here, certain observations are discussed relating the 5' end and the loop III of tRNA to the function of tRNA in this process. In addition, there appears to be certain correlations between these portions of tRNA molecules and the group structure of amino acids revealed in the genetic tableau.

**TH-PM-F9** THE SEDIMENTATION BEHAVIOR OF CLOSED AND OPEN DNAs IN AQUEOUS ALKALI TRICHLOROACETATES. R.L.Burke* and W.R.Bauer* (Intr.by M.Riley), Dept. of Microbiology, S.U.N.Y. at Stony Brook, N.Y. 11794.

Aqueous RbTCA is suitable for buoyant banding of both the duplex and the denatured forms of DNA at room temperature and neutral pH. For the nicked circular DNA (DNA II) from bacteriophage PM-2 the native form is buoyant at 25° at 3.30M salt, whereas the denatured, separated strands band together at 4.44M. The virion closed circular PM-2 DNA (DNA I) is buoyant at 3.38M at 25° and separates completely from II. We have investigated the buoyant behavior of a family of closed circular DNAs of increasing negative superhelix density prepared by treating I with the DNA relaxing protein from HeLa nuclei in the presence of ethidium bromide followed by removal of dye. A plot of buoyant density versus the superhelix density measured in ethidium bromide/CsCl yields a straight line, suggesting that the buoyant shift between the closed and nicked circles in RbTCA is due to the early melting associated with the removal of all initially present superhelical turns. From the slope of this curve we calculate that the superhelix density of PM-2 DNA I is 0.094 in this solvent, leading to the estimate of 22.7° for the ethidium bromide unwinding angle. Melting curves for bacteriophage DNAs PM2 II, T7 and $\lambda$ in RbTCA and NaTCA show monophasic transitions with breadths of 4-6°C. We have monitored the helix-coil transition of the early melting of PM2 DNA I by band sedimentation in both solvents. The melting of the early region is noncooperative and occurs over a broad salt range up to 3.0M at 25°C. The sedimentation coefficient ratio of the closed to the nicked DNA varies from a limiting value of 1.37 in low salt to 1.00 in the region of 3M TCA. PM-2 DNA II melts cooperatively at approximately 3.2M-NaTCA in the sedimentation velocity experiments, a salt concentration identical to that which produces the optical helix-coil transition of this DNA at 25°.

**TH-PM-F10** NEUTRAL SUCROSE SEDIMENTATION OF BACTERIAL DNA WITHOUT SUCROSE OR ROTOR-SPEED ARTIFACTS. R.W. Clark,* and C.S. Lange, Departments of Radiology, Radiation Biology and Biophysics, University of Rochester School of Medicine & Dentistry, Rochester, N.Y. 14642.

A system for studying native DNA sedimentation in the zonal rotor has been developed. Isokinetic neutral sucrose gradients of the type described by Noll have been designed for the Ti-15 zonal rotor, enabling the calculation of sedimentation coefficients ($S_{20,w}$) from the conditions of centrifugation (distance sedimented, gradient geometry and $\omega^2 t$). Bacteriophage DNA from T7 and T4 have been sedimented on these gradients and the resultant $S_{20,w}$ values are in agreement with sedimentation coefficients measured in salt solutions in the analytical ultracentrifuge (T7 = 32.4, T4 = 61.6). These experiments do not confirm a previous report (Levin & Hutchinson, 1973) of anomalous DNA sedimentation on sucrose. Based on the measured values of $S_{20,w}$ for T7 and T4 and the best estimates of their molecular weights (Freifelder, 1970) an equation relating $S_{20,w}$ and molecular weight has been derived ($S_{20,w} = 0.0223M^{0.428}$). Preliminary results from the sedimentation of Bacillus subtilis DNA in the zonal rotor show molecules which sediment at about 210 $S_{20,w}$. Calculating molecular weight with the above equation gives a value of 2 x $10^9$ daltons, which agrees with the viscoelastometer based estimate of Klotz & Zimm (1972). This sedimentation coefficient of 210 has been measured over the range of 10 to 20 kRPM and no indication of Zimm-type speed dependence has been detected. This result agrees with an earlier report of the absence of speed dependence in the zonal rotor (Wheeler, 1974). This paper is based on work performed under contract with the U.S. Energy Research & Development Administration, in the Department of Experimental Radiology (Contract No. AT(30-1)-4284), and the University of Rochester Biomedical and Environmental Research Project and has been assigned Report No. UR-3490-849.

**TH-PM-F11** A GENERAL METHOD FOR SELECTIVE STAINING OF POLYNUCLEOTIDES WITH HEAVY METALS FOR SEQUENCING IN THE ELECTRON MICROSCOPE. K. Strothkamp* and S.J. Lippard, Department of Chemistry, Columbia University, New York, N.Y. 10027

Platinum binding to nucleoside phosphorothioates has been examined by spectroscopy, electrophoresis and ion-exchange chromatography. Aquoterpyridineplatinum(II) nitrate, $[(terpy)Pt(H_2O)](NO_3)_2$, forms a 1:1 adduct with uridine monophosphorothioate. UV and NMR spectroscopy indicate that the nucleotide is coordinated to platinum through the sulfur atom. As judged by the UV spectra, $[(terpy)Pt(H_2O)]^{2+}$ binds to poly r(A $\underline{s}$ U) and poly r($\underline{s}$ A $\underline{s}$ U) through sulfur. With poly r(A - U), a slower reaction occurs at the bases. After reaction with chloroterpyridineplatinum(II), poly r(A $\underline{s}$ U) and poly r($\underline{s}$ A $\underline{s}$ U) no longer migrate as anions in electrophoresis. The migration of poly r(A - U) is not altered under the same conditions. Tritiated $[(terpy)Pt]^{2+}$ bound to poly r(A $\underline{s}$ U) is not retained on a cation exchange resin which removes the complex from poly r(A - U). The present results demonstrate the ability of the nucleoside thiophosphate group to bind platinum, and presumably other class B heavy metals, selectively in a polynucleotide. A previous study reported quantitative incorporation of thiophosphate groups into polynucleotides adjacent to a specific base (F. Eckstein and H. Gindl, Eur. J. Biochem., 13, 558-564 (1970)). The use of heavy metal labeled thiophosphate groups for the sequencing of nucleic acids by electron microscopy therefore appears feasible. A major advantage of this approach is use of the same chemistry for labeling all the bases.

We thank Dr. F. Eckstein for helpful discussions and for samples of phosphorothioate substituted RNAs.

**TH-PM-F12** TEMPLATE EFFECTS OF CIS AND TRANS DICHLORODIAMMINE PLATINUM ON POLY dAT:dAT AND POLY dA:dT. H.C. Harder, Pharmacology Dept., George Washington Univ., Washington, D.C,20037 R.G. Smith*, NIH, Bethesda, Md. 20014.

Cis-dichlorodiammine platinum (cis), a new antitumor agent, causes interstrand DNA cross-links as does the inactive trans isomer. We investigated the possible biological significance of reactions of cis, trans and monofunctional [diethylenetriaminechloro platinum] chloride (dien) with the polynucleotides dAT:dAT and dA:dT by assaying template-primer activity with DNA polymerase α and β partially purified from normal human lymphocytes (8402 and 1788 respectively). The $r_b$-50 (moles of bound platinum/mole base nucleotide required to decrease template activity by 50%) for cis treated dAT:dAT using β was 0.003 while that for trans was 0.021. The kinetics of dAT:dAT template inactivation by dien were identical to that of trans, suggesting that dAT:dAT template inactivation by trans is caused solely by monofunctional reactions. With dA:dT the only bifunctional reactions would be intrastrand because these compounds do not react with thymine. With $^3$H-dTTP incorporation by β, only cis inhibited the template activity of dA:dT; trans and especially dien enhanced the template activity. Here only the dA strand was being copied. However when only the dT strand is replicated using $^3$H-dATP as the incorporation label, all 3 compounds enhanced the activity in the order cis>dien>trans just opposite the ordering observed with $^3$H-dTTP. When the dA:dT treated templates were tested with α, $^3$H-dTTP incorporation was inhibited in the order dien>trans>cis, but $^3$H-dATP incorporation was enhanced in the same order. The denaturation properties of the Pt compounds may be partially responsible for the enhanced template activity. However this cannot explain why inhibition is observed with α while enhancement is observed with β unless it is related to the cellular role of these enzymes, i.e. normal vs. repair replication.

This research was supported by American Cancer Society grant CI-107 and NCI grant CA-02978.

TH-PM-G1 IDENTIFICATION OF THE PHOTOSENSITIVE PIGMENT IN THE GIANT NEURON OF APLYSIA CALIFORNICA. L. A. Sordahl, A. Lewis, J. Pancurak*, A. M. Brown and G. Perreault*. University of Texas Medical Branch, Galveston, Texas 77550 and Cornell University, Ithaca, New York 14850.

Phototransduction in Aplysia neurons is probably mediated by the release of calcium from cytoplasmic pigmented granules called lipochondria. The exact nature of the pigment is unknown. A lipochondria-enriched granule fraction was isolated from Aplysia giant neurons and examined by split-beam spectrophotometry and resonance Raman spectroscopy. The absorbance spectrum of the isolated intact granules revealed absorbance maxima at 413, 433 and 459 nm. Subsequent extraction of the lipochondria pigment into petroleum ether showed absorbance maxima at 425, 447 and 475 nm which are very similar to β-carotene. Resonance Raman spectroscopy of the intact granules and the ether extracts of pigment exhibited Raman spectra with major peaks at 1006, 1159 and 1528 $cm^{-1}$ which is almost identical to β-carotene dissolved in petroleum ether. It is important to note that resonance Raman spectroscopy obtained on a single, intact R-2 neuron exhibited identical vibrational frequencies as those obtained with isolated lipochondria and the petroleum ether extracts of pigment. These results indicate the photosensitive pigment localized in Aplysia neurons is not a "rhodopsin-like" molecule, but appears to be β-carotene. (Supported by NIH grant NS-11453 and by NSF EPP 75-09129 and NIH EY 01377 grants to A. Lewis, who is an Alfred P. Sloan Fellow.)

TH-PM-G2 FACTORS CONTRIBUTING TO "LATCH-UP" OF THE RECEPTOR POTENTIAL IN A GIANT PHOTORECEPTOR. L. Monti-Bloch*, H. Mack Brown, and James H. Saunders, Department of Physiology, University of Utah College of Medicine, Salt Lake City, Utah, 84132.

Illumination of green-adapted Balanus eburneus lateral photoreceptors with red light produces a membrane depolarization that persists in darkness (latch-up), which is associated with an inward current whose ionic mechanisms are similar to those occurring during illumination with white light (H.M. Brown,et.al.). The amplitude and duration of latch-up depend on the intensity, duration, and wavelength of the priming (green) and inducing (red) flashes and on the duration of the dark interval (D.I.) between them. A model of latch-up (Hochstein,et.al.) accounts for two observations: 1) red light does not usually produce latch-up unless the photoreceptor has been blue-adapted, 2) blue-green light terminates latch-up or prevents its induction; in terms of this model these phenomena are due to an inhibitor evoked by blue-green light. We observe that: 1) 530-540 nm light is more efficient than 480-495 nm light as a priming flash, 2) latch-up depends on priming flash intensity and duration, 3) the time course of latch-up induction on the order of minutes rather than seconds as observed by Hillman, et.al. for inhibition, and 4) D.I. between the 530 nm and the 602 nm flashes influences the duration of latch-up. This suggests that an excitatory precursor accumulates in the dark following the priming flash and that latch-up duration reaches a maximum limited by the amount of precursor formed during the first 30 minutes after stimulation with green light. Duration of latch-up is dependent on the amount of precursor formed during the D.I., rather than on the formation of an inhibitor with a different wavelength maximum and time course. (Brown, Cornwall, J. Physiol., 248 (1975) 555 and 579; Hochstein, Minke, Hillman, J. Gen. Physiol. 62 (1973) 105.

TH-PM-G3 COLOR DEPENDENT POTENTIAL CHANGES OF OPPOSITE POLARITY IN SINGLE VISUAL RECEPTORS OF PECTEN IRRADIANS. M. Carter Cornwall and A.L.F. Gorman, Department of Physiology, Boston University School of Medicine, Boston, Mass. 02118

White light evokes a hyperpolarizing response in the distal photoreceptor cells of the scallop retina. This response is characterized by a fast onset to a peak which decays to a plateau, and a fast after-depolarization that often overshoots the dark potential. Our recent experiments show that the response to white light is a complex waveform composed of wavelength dependent potential changes of opposite polarity. A step of blue light ($\lambda < 500$ nm) produces rapid hyperpolarization to a plateau, and a slow return to the dark potential, without an after-depolarization. When a red step ($\lambda > 560$ nm) is given during the hyperpolarization produced by a blue light, a depolarization results which can overshoot the dark potential. Alone, a step of red light produces a small, transient hyperpolarization, a decay of membrane potential to a level more depolarized than the dark potential and a large depolarization at light off. A step of blue light presented on a red background results in a rapid hyperpolarization at light on, a return to the pre-flash membrane potential at light off, but no after-depolarization. The hyperpolarization produced by flashes of blue light is associated with a negative early receptor potential (ERP) whereas the depolarization produced by red light is associated with a positive ERP. Our results suggest that more than one pigment or pigment state is involved in the control of membrane potential in this photoreceptor. This research supported by NIH grant EY01157.

**TH-PM-G4** IONIC MECHANISM OF COLOR DEPENDENT MEMBRANE RESPONSES OF OPPOSITE POLARITY IN SINGLE PHOTORECEPTORS OF PECTEN IRRADIANS. A.L.F. Gorman and M. Carter Cornwall, Department of Physiology, Boston University School of Medicine, Boston, Mass. 02118

We have previously shown that the membrane hyperpolarization to white light in the distal cells of the scallop Pecten irradians is associated with an increase in membrane permeability to $K^+$ ions. Our recent results suggest that the hyperpolarization produced by flashes of blue light given on a red background have properties identical to those produced by white light, i.e. increased membrane conductance and a reversal potential which is more negative than dark membrane potential. Flashes of red light presented on a blue background produce membrane depolarizations which are also associated with increased membrane conductance, but the reversal potential of the depolarizing response (estimated from current voltage plots) is more positive than the membrane potential in darkness. External $Na^+$ concentration was reduced by substituting large cations (choline or Tris). Plots of the peak depolarization at different external $Na^+$ concentrations show that the amplitude of the depolarizing response decreases as the external $Na^+$ is reduced and is abolished by its complete removal. Our results suggest that red light may increase membrane permeability to $Na^+$ ions. These experiments, however, do not reveal the extent to which $Na^+$ or $K^+$ permeability decreases may be involved in hyperpolarizing and depolarizing responses respectively. This research supported by NIH grant EY01157.

**TH-PM-G5** STIMULATED CONDUCTIVITY (THRESHOLD SWITCHING) IN ISOLATED PHOTORECEPTOR MEMBRANES. P. Proctor*, D. Kirkpatrick, J. McGinness*, and P. Corry*, Dept. of Ophthalmology, Baylor College of Medicine, and Dept. of Physics, U. T. Cancer Center, Houston, Texas 77025.

The current/voltage characteristics of a mildly hydrated (8-10%) 0.9 mm thick pellet of isolated bovine photoreceptor membranes were determined by applying a ramped 200 msec. voltage pulse with a peak at 500 volts. The material exibited an abrupt and reversible manyfold increase in conductivity, i.e., threshold switched, at a threshold potential Vt = 340 v. A similar pellet of isolated photoreceptor phospholipid also threshold switched, but only after repeated pulses and at higher threshold potential. Phospholipid isolated from red cell membranes threshold switched, while soybean lecithin did not switch, even in the presence of 2% all-trans retinal, suggesting that the degree of unsaturation of the lipids is a key parameter for threshold switching. The significance of these results is that threshold switching is a known subset of stimulated conductivity, which is a special property of some amorphous semiconductors. Stimulated conductivity arises out of the disorder of a material and probably occurs when electrons in localized traps are promoted energetically, e.g., by light or an electric field, to an overlying delocalized conduction band (viz., in photography and in the xerographic process). Thus, threshold switching indicates that the photoreceptor membrane is an amorphous semiconductor and further suggests a possible role for electron-phonon interactions and stimulated conductivity in photoreceptor function. Supported by the Retina Research Foundation, Houston, Texas.

**TH-PM-G6** ON THE FUNCTION OF MUTUAL INHIBITION IN VISUAL INFORMATION PROCESSING IN LIMULUS. F.A.Dodge, E.Kaplan†, F.Ratliff†, H.K.Hartline, Rockefeller University, New York 10021

Preliminary experiments analyzing the patterns of visual excitation and of retinal activity in a Limulus moving freely in a shallow bay suggests that the lateral eye selectively transmits information about features in the visual environment because mutual inhibition suppresses common-mode signals. Visual space was sampled by a photocell behind an optical guide which had the same acceptance angle as a single ommatidium. Spectral analysis as the crab walked on sand showed that they are predominately slow (80% of power less than 2 Hz). Spectral analysis of single unit spike-rate fluctuations confirmed that inhibition greatly attenuated low frequencies. Spike-rate fluctuations of a pair of units with overlapping acceptance angles are positively correlated, but negatively correlated for wide divergence. Since the fluctuations due to the crab's motion were typically much larger than those due to waves, we conclude that the natural stimulus results from scanning visual space with low amplitude, irregular oscillations. If we abstract the visual environment (below the horizontal) to the sum of a slow gradient and an edge, then such scanning generates synchronous excitation (E) whose amplitude is augmented for those ommatidia seeing the edge. The computed response (R) to this simple pattern shows that mutual inhibition effectively suppresses the common mode component, while the population transmits signals generated by the edge.

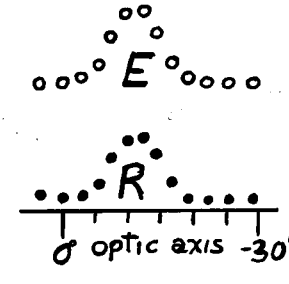


Supported by Grants NIH-EY188 and NSF-GB36168

**TH-PM-G7** CRYSTALS AND PHOTORECEPTORS. Jerome J. Wolken. Biophysical Research Laboratory, Carnegie-Mellon University, Pittsburgh, Pa., 15213.

The search for evolutionary clues to the development of the visual photoreceptors of the eye has led to a study of photoreceptor structures and pigments in microorganisms. Here, I would like to present our researches on the bacterium Halobacterium halobium, the fungus Phycomyces blakesleeanus, and the protozoan algal flagellate, Euglena gracilis. These organisms appear to have developed photoreceptors; for example, the Halobacterium halobium cell membrane has within it a "purple membrane" which is a crystalline structure containing a visual pigment whose chromophore is retinal, found in all animal eyes. Similarly, within the growth zone of Phycomyces there is a crystalline photoreceptor which is involved in its phototropism. In Euglena there is a crystalline structure associated with the flagellum, a photoreceptor system for phototaxis. The photoreceptor molecules in these structures are complexes of carotenoids, and/or a flavin with a specific protein to form a pigment-protein complex, a rhodopsin or a flavoprotein. Phycomyces and Euglena also possess an interesting chemistry: for example, acetylcholine, acetylcholinesterase, and an ATP-ATPase system, which function in neuro- and muscular systems of animals. How such crystalline structures may have given rise to the more highly evolved photoreceptor lamellar structures of animals will be explored using as models these unicellular organisms.

Supported in part by the Penna. Lions Sight Conservation and Eye Research Foundation, Inc.

**TH-PM-G8** VOLTAGE CLAMP STUDIES OF IDENTIFIED APLYSIA INTERNEURON $L_{10}$. M.C. Andresen* and A.M. Brown, Department of Physiology and Biophysics, University of Texas Medical Branch, Galveston, Texas 77550.

Light-induced potential and current changes were examined in the identified Aplysia interneuron $L_{10}$ using current and voltage clamp. As with the light responsive $R_2$ giant neuron of Aplysia, $L_{10}$ is a deeply pigmented, orange-red color. Five-second light flashes produced hyperpolarizations in $L_{10}$ of up to 20 mV and conductance increases of 20% using constant-current pulses. Under voltage clamp, similar stimuli produced peak outward currents of 8-10 nA. The light-induced current responses ($I_L$) to brief flashes (50-100 msec) began after a latency of about 100 msec, peaked at 5 secs and returned to zero current levels within 30 secs. In response to prolonged "steps" of illumination (up to 9 min duration), $L_{10}$ exhibited an initial outward current which adapted to a lower steady state level This level was then maintained for the duration of the stimulus. The $I_L$ dose-response relationship for 470 nm monochromatic light in 100 msec pulses had a threshold of $10^{14}$ Q/cm$^2$ and was saturated at 2 X $10^{16}$ Q/cm$^2$. The light sensitivity of the $L_{10}$ was at least two orders of magnitude greater than $R_2$. Criterion response and equal energy action spectra showed a maximum sensitivity at 470 nm. The $I_L$ response declined in magnitude at increasingly hyperpolarized holding potentials, until at potentials greater than -80 mV it disappeared. If cells were held at the resting potential and, at the time of the peak light current, were stepped to a new holding potential, $I_L$ reversed sign at potentials greater than -85 mV. Measurements of the light transmission through the body wall showed that sufficient light may enter to hyperpolarize this interneuron by several mV, thereby interrupting its normal autoactive spiking pattern.

**TH-PM-G9** COMPARISON OF FREQUENCY RESPONSES OF ERG COMPONENTS IN WILD-TYPE AND MUTANT DROSOPHILA. Fulton Wong* and Chun-Fang Wu* (Intro. by William L. Pak), Rockefeller Univ., New York 10021 and Dept. of Biological Sciences, Purdue Univ., Lafayette, IN 47907

The electroretinogram (ERG) of Drosophila compound eye consists of contributions from receptor cells and the second order neurons in the lamina. Each ommatidium has three types of receptors: $R_{1-6}$, $R_7$ and $R_8$. The lamina receives input from $R_{1-6}$, while $R_{7,8}$ by-pass it and project onto the higher visual center. The ommochrome granules in the receptor cell body are known to migrate in response to light thus limiting the amount of light entering the rhabdomere. Comparison between the frequency responses of the wild type and the mutant lacking the ommachrome granules indicates that the pigment migration reduces the amplitude gain at frequencies below 0.5 Hz, consistent with the reported migration time constant of 2 sec. The mutant with defective lamina or those in which only $R_{7,8}$ or $R_8$ is functional showed a high frequency cutoff with a corner frequency of 15-25 Hz; while in wild type the frequency response peaked at about 20 Hz. These results suggest that the lamina contributes mainly to the high frequency components of the transfer function. As in many other arthropods, the receptor potential of Drosophila consists of a summation of small discrete potentials known as bumps. In the mutant in which the bumps exhibit a dispersed latency distribution in response to a dim flash, the receptor showed a poor high frequency response, the corner frequency being lowered to about 3 Hz. The slope of the cutoff was approximately 20 db/dec indicating that the latency dispersion in this mutant is the major limiting factor in temporal resolution. Light-evoked high frequency oscillations have been observed in the ERG of another mutant. The oscillation was found sharply tuned to light flickering at about 50 Hz; the phase plot of the transfer function also showed the expected behavior of an ideal resonator. Supported by NIH grants EY00188-20 to Floyd Ratliff & EY00033-07 to W.P.

**TH-PM-G10** SLOW STRESS RELAXATION OPPOSES SENSORY ADAPTATION IN A MECHANORECEPTOR OF THE INSECT EXOSKELETON. Judith L. Mosinger* and K.M. Chapman, Neurosciences Section, Div. Biol. & Med. Sciences, Brown University, Providence, RI, USA 02912

The proprioceptive campaniform sensilla of the insect leg, which sense exoskeletal strain in the coordination of posture and walking, adapt slowly and completely to experimentally applied punctate stimuli. The major component of adaptation occurs in impulse initiation at the axonal encoder, but the receptor potential also adapts to applied force (Mann & Chapman, Brain Res. 97: 331-336, 1975). Punctate forces indent a cuticular cap and deform the dendrite of the receptor's single bipolar sensory neuron. If this mechanical coupling were time dependent, it would make a third, explicit contribution to the over-all time dependence of the receptor. We have therefore measured the frequency response of cap compliance using sinusoidal forces of 0 - 50 μN on the range 3 mHz to 100 Hz, as described by Chapman & Duckrow (J. Comp. Physiol. 100: 251-268, 1975). Unlike impulse frequency and generator current, the compliance, typically 1 - 10 nm/μN, decreases with frequency with a power coefficient of about -0.2 and indentation lagging force by about 20°, in the manner of a viscoelastic polymer with widely distributed relaxation coefficients. Thus slow stress relaxation of the cap cuticle tends to oppose the adapting contributions of generator current and impulse initiation, and the sensory response adapts somewhat more rapidly to indentation than to force.

**TH-PM-G11** A PHYSICO-CHEMICAL MODEL OF THE STIMULATION OF TASTE RECEPTOR CELLS BY SALT. John A. DeSimone and Steven Price*, Department of Physiology, Medical College of Virginia, Richmond, Virginia 23298

A taste cell mucosal surface is regarded as a planar region containing bound anionic sites and openings to ionic channels. It is assumed that the bulk aqueous properties of the exterior phase are not continuous with the surface, but terminate at a plane near the surface. The region between the (Stern) plane and the membrane is regarded as having a lower dielectric constant than bulk water. This fact admits the possibility of ion pair formation between fixed sites and mobile cations. Mobile ion pairs entering the region may also bind to a fixed anionic site. Thus, it is assumed that mobile cations and ion pairs are potential determining species at the surface. Binding cations neutralizes surface charge, whereas binding mobile ion pairs does not. This competition accounts for the observed anion effect on stimulation of taste receptors by sodium salts. The potential profile is obtained by solving Laplace's equation in the Stern region and Poisson's equation for the aqueous phase. The complete potential profile is constructed by superimposing this phase boundary potential (and another one obtained at the cell inner surface) with an ionic diffusion potential across the membrane. The model accounts for the anion effect on receptor potential, pH effects, the reversal of polarity when cells are treated with $FeCl_3$ and the so called "water response", depolarization of the taste cell upon dilution of the stimulating solution below a critical lower limit. The proposed model does away with the necessity for both bound cationic and anionic receptors, and further suggests that limited access to a Stern-like region continuous with membrane channels may generally serve to control transport of ions.

**TH-PM-G12** FREQUENCY RESPONSE CHARACTERISTICS OF NORMOTENSIVE AND HYPERTENSIVE AORTIC BARORECEPTORS. F.H. Tuley, A.M. Brown and W.R. Saum*, Department of Physiology and Biophysics, University of Texas Medical Branch, Galveston, Texas 77550.

The responses of individual aortic baroreceptors to step and sinusoidal pressures applied to the aortic arch have been examined in normotensive (NTR's) and spontaneously hypertensive rats (SHR's). Arterial blood pressures of each animal were determined for at least one week prior to experiment. Steps were applied from threshold to saturating levels of discharge. The pressure-response curves of SHR's showed higher thresholds and lower sensitivities for both transient and steady-state discharge. The instantaneous frequency response to a step input of pressure was shown to be fitted by a sum of three exponentials which are similar for NTR's and SHR's. From the amplitudes and phases of response to sinusoidal modulation of the pressure input a quantitative input-output relationship, in the form of a transfer function, was determined. Peak amplitude value in the frequency domain calculated thus far range from 2 to 5 Hz. These results agree with values calculated from the step-response data. Differences between NTR and SHR baroreceptors have not been demonstrated to this point.

**TH-PM-G13** COCHLEAR FLUID MECHANICS CONSIDERED AS FLOWS ON A CUSP CATASTROPHE.
T.W. Barrett, Department of Physiology & Biophysics, University of Tennessee Center for the Health Sciences, Memphis, TN 38163

The elementary signal of sound[1] is the result of potential minimization[2], when the potential is the unfolding of an equivalent class of neighborhood functions, and occurs at a critical point[3], or at a singularity in mapping one manifold into another[4]. In these terms an elementary signal is caused by an unstable mapping of a potential function (i.e., a cusp catastrophe[2]), resulting in a limit cycle[5]. In that the movements of cochlear fluids elicited by an elementary signal are diffeomorphic to the representation of an elementary signal determined by the minimization of a potential, a description of those movements may be considered as flows on a cusp catastrophe[2]. The result of this analysis is a new insight into auditory signal processing. A new deterministic foundation for quantum physics in general is also indicated.

[1]Barrett, T.W. Acustica 33 (1975) 149; Acustica 33 (1975) 102; J. Acoust. Soc. Am. 54 (1973) 1092; Biophysical Soc. Abs (1973), (1974), (1975).
[2]Thom, R. "Structural stability and morphogenesis" (1975) Benjamin, Reading, Mass.
[3]Morse, M. Trans. Am. Math. Soc. 27 (1925) 345; 33 (1931) 72.
[4]Whitney, H. Ann. Math. 45 (1944) 220 & 247; 62 (1955) 374.
[5]Van der Pol, B. Philos. Mag. 2 (1926) 978.

**TH-PM-G14A** PROBE FOR MAKING IN VIVO RETINAL OPTICAL MEASUREMENTS.
F.M. Loxsom, J. Crawford*, and D. Nawrocki, Physics Department, Trinity University, San Antonio, Texas, and Physics Department, Southwest Texas State University, San Marcos, Texas, and Technology Inc., San Antonio, Texas.

An optical probe suitable for making optical measurement at the retinal level has been designed, constructed and used as a diagnostic tool in studies involving the interaction of coherent light with the retina. The probe consists of two major components. A single 2mm diameter glass rod has been pulled on an microelectrode puller to form a tip of less than 100μ. This probe was coated by vacumm deposition with a thin film of aluminum. When the ends were cleaned, this probe was used to conduct light to a very sensitive photodiode/op-amp unit. The directional sensitivity of this probe is such that only light within a $\sim 20^0$ cone is easily transmitted. The probe has proved useful in determining mechanical stability, beam width, and other optical parameters in the primate retina. This research was supported in part by a NSF Faculty Research Participation Program and by USAF contract, F41609-73-C-0071.